Towards Wireless Control in Industrial Process Automation

Anders Ahlén, Johan Åkerberg, Markus Eriksson, Alf J. Isaksson,
Takuya Iwaki, Karl Henrik Johansson, Steffi Knorn,
Thomas Lindh, and Henrik Sandberg
POC: A. Ahlén (anders.ahlen@signal.uu.se)
June 4, 2019

Wireless sensors and networks are today only occasionally used in control loops in the process industry. With the current rapid developments in embedded and high-performance computing, wireless communication, and cloud technology, drastic changes in the architecture and operation of industrial automation systems seem more likely to happen than ever before. These changes are driven by ever growing demands on production quality and flexibility. However, there are several research obstacles to overcome: The radio communication environment in the process industry is often troublesome as the environment is frequently cluttered with large metal objects, moving machines and vehicles, and processes emitting radio disturbances [1], [2]. Successful deployment of a wireless control system in such an environment requires careful design of communication links and network protocols, as well as robust and re-configurable control algorithms.

Based on some examples from the Iggesund paper mill in Sweden, with a long history, see "Iggesund Mill History", we will in this paper discuss some recent developments towards wireless control in industrial process automation. Despite major scientific progress over the last couple of decades in wireless networked control [3] with, for instance, important results on how plants can be stabilized and optimized over packet-switched networks [4] surprisingly little impact has been reported on commercial implementations in the process industry. We argue here that a more integrated approach to the design of these systems is needed, exploring trade-offs between the communication and control systems in a systematic way. Existing standardized industrial communication protocols, such as ISA-100 and WirelessHART, provide a large degree of freedom for the users including many tuning parameters, but developing co-design methods utilizing this freedom is still needed [5]. A brief survey of recent advances on wireless control is summarized in "Advances in Wireless Control".

The outline of this paper is as follows. First we describe a possible future control architecture and detail some key challenges in next generation process automation. The Iggesund paper mill is then introduced as a case study. It is used throughout the paper to illustrate the considered communication and control problems. Results are presented on modelling of radio channels in an industrial environment. The joint behaviour of multiple wireless sensor–sensor and sensor–gateway channels is discussed and models useful for routing data packets are proposed. Energy harvesting in wireless sensor networks is then demonstrated on the industrial process. Event-based control for wireless systems is investigated for both feedback and feedforward control, followed by a proof-of-concept implementation of wireless control at Iggesund. Finally, in the last section, conclusions are drawn.

Challenges in next generation process control

With the recent developments towards Internet-of-Things (IoT), we can expect that future devices and systems can much more seamlessly communicate. The most immediate effects are seen in data analytics, where new devices can collect data online and feed it into the cloud without going through a control system. Once in the cloud almost "unlimited" computing power can be applied for processing the data for various purposes such as, for instance, predictive or prescriptive maintenance. It is, however, clear that this will have an effect not only on analytics but also on process control and other process operations.

Inspired by the development in mobile platforms such as iPhone and Android it is reasonable to assume that most functions that are not time- or safety critical could become available as "apps" in an automation platform. Today we often have large monolithic software systems for each layer of the classical automation pyramid, such as for process control, manufacturing execution system (MES), and enterprise resource planning (ERP). Instead, these functions may be broken down into smaller components that seamlessly communicate within one "app" platform. This would also make it easier for smaller players who only provide a limited or smaller scope of functionality to participate in the market.

ExxonMobil, as one of the world's largest process companies, in 2016 clearly communicated its vision towards a future control architecture through a set of presentations [6]. Their vision states concretely that a future control system should be built on distributed control nodes (DCN) that are dedicated single-channel I/O modules with control capability connected to a real-time data service bus. Furthermore, the operations platform should be open and use open-source software. This would enable a much easier revamping of current distributed control system (DCS) architecture philosophy, which in their view is both complex and expensive. By adopting this vision, together with the above idea of one common "app" platform, the traditional automation

pyramid, which structurally separates process control, scheduling and planning to their own hierarchical levels, may be replaced by a more flexible paradigm. A somewhat simplified version of the ExxonMobil vision is depicted in Figure 1.

At the lowest level of a control system, there are measurement devices, for instance, sensors and analyzers, as well as actuating devices such as valves and pumps. At this device level the connection to the common real-time bus could be realized through a standardized DCN as suggested by ExxonMobil. More futuristic, however, is to assume that all devices have enough intelligence to handle the connectivity and low level control computations themselves, see, for example [7]. As indicated already above, one interesting question is then where a particular computation should take place. Clearly there will always be a need to carry out some computations with a minimum of latency. Hence we have a trade-off between moving current DCS functionality to the Operations Platform or the DCN/device, as indicated by the arrows in Figure 1.

In this whole discussion a central question to this paper is what role wireless communications will play in this future automation architecture. In Figure 1, the possibility of a wireless gateway is indicated. However, we will in this paper argue that a standard choice for the DCN and other intelligent devices would be to use wireless communications, even for situations requiring fast communications. As has been pointed out by many before us [2], [8], [9], there are multiple potential advantages with wireless instead of wired communications such as cost savings in cables and installation as well as more flexible operation. The rest of this paper will be devoted to investigating the feasibility and reliability of the use of wireless communications in process applications with a particular focus on the pulp and paper industry.

From a system perspective there are also several challenges in order to maintain high availability and safe control functions. From an engineering perspective the control applications have to support online changes and the system architecture needs to deal with seamless reconfiguration, to distribute new applications while ensuring system integrity to name a few. Furthermore, on the real-time bus, new challenges arise in order to deal with different real-time traffic classes, video streams, as well as best-effort traffic in a system architecture such as the one in Figure 1. In addition to this, redundancy is required in order to meet the industry demand on the availability of the control system, and to take the processes into safe states in case of errors that cannot be automatically recovered, without creating isolated network functions that are executing (partly) blindly.

Iggesund paperboard machine case study

The Iggesund Mill is a fully integrated pulp and paperboard mill with a long history, see "Iggesund Mill History". The pulp mill is the area where the large chimneys are located, in the upper center of Figure 2. The paperboard mill and the coating kitchen is the building complex in the middle of Figure 2. There are two paperboard machines, see Figure 3, and the products that are manufactured are primarily for packaging and graphic purposes, which require high quality. In order to obtain a paperboard of the quality produced at the Iggesund Mill, there is also a coating kitchen that delivers coatings which are used to coat the paperboard to make it smooth and even, and hence a good surface for printing.

Throughout a recent three year long project period, several real live tests have been conducted to evaluate wireless control in the industrial environment of the factory. These tests were carried out mainly at the coating kitchen, where there are two starch cookers. The starch production is one important ingredient when mixing and preparing the coating of the paperboard. The starch is providing the finish and color of the paperboard which is used for exclusive packaging of, for example, whiskey, perfumes, and chocolate. This process is delivering coating to both paper machines and the final quality of the paperboard is depending on a constant supply of high quality coating. The cookers are used to boil the starch, which is subsequently used in the manufacturing of the different coatings. During the experiments, only one cooker was used. The main reason for using only one of the boilers as a test bed in the wireless control experiments was that we could implement the wireless outbreak on one cooker while in the meantime continue with normal production on the other, and thus the experiments did not disturb the production at the paperboard machines. The process in the cookers works so that silo H1 is a buffer for the starch powder. A picture of the silo H1 is shown in the upper left part of Figure 4. From there, the powder is transported to a storage hopper with a level regulator to ensure the same degree of filling in the dosing screws. It is in the mixing tank the dry powder mixes with water. The picture at the bottom left part of Figure 4 shows this process, which is controlled via a concentration regulator. The mixture is then pumped into the steam ejector where steam is added to boil the starch. The starch boiling process is controlled by a temperature regulator. After that, water is added again to get the correct dry content on the final product. A picture of the process where the starch is boiled is shown in the upper right corner of Figure 4. The starch cooking is a batch process which is started and stopped automatically by the level in the storage tanks. The picture at the bottom right of Figure 4 shows these storage tanks.

A wireless control architecture for the starch cooker

Figure 5 shows a proposed wireless control architecture for the starch cooker process of the Iggesund pulp and paperboard mill. The architecture consists of multiple wireless feedback loops involving sensors (S_j) and actuators (A_j). From left to right in Figure 5 the cooker works as follows: Water from the mix water tank, the level of which is controlled by (S_1, A_1), is mixed with starch powder distributed through the mix funnel. The properties of the so obtained starch-water mixture is governed by the concentration control loop (S_2, A_2) and the coarse flow control loop (S_3, A_3). The mixture is cooked using a steam injector, which is temperature controlled by (S_4, A_4). The concentration of the starch solution is further diluted by the fine flow control loop (S_5, A_5) after which a mixing and pressure control loop, governed by (S_6, A_6), is making the final touch before the starch solution is sent to the storage tank. In our wireless setup, all control actions are calculated at the actuators in a distributed fashion and the sensor- and actuator information is sent to the gateways (GW) for further distribution to the operators.

Modeling of radio channels in industrial environment

When a wireless environment is static, the wireless link design is fairly straightforward, even if Line-of-Sight between the transmitting node and the receiving node cannot be obtained. It is then just a matter of selecting the appropriate number of sensor nodes, good locations and/or adjusting the transmit power. However, even if an industrial environment at a first glance looks static, it is very seldom so over a longer time horizon (several minutes and hours).

In the literature, typical indoor channels are found to be well described by either log-normal (LN), Rayleigh, Rice, Nakagami-m, (Gamma (G) in the power domain), or, sometimes, even Weibull distributions [1], [10]–[12]. The distribution that fits the received data best depends on the environment and the degree of motion around the communicating sensor nodes and the observation interval. For a comprehensive overview of radio channel characteristics in indoor and industrial environments, see, for example., [11]–[13] and the references therein. Furthermore, previous studies have observed that temporal channel variations in WSNs with stationary nodes, that is, both the transmitting and receiving antennas are stationary, typically follow a Rician or Nakagami-m distribution [1], [11], [14].

Characterizing channel gain variability

To obtain an accurate representation of the radio environment at the paper mill in Iggesund, numerous point-to-point measurements were performed at different positions along the paper mill production line as well as in the starch cooker environment. In addition to these point-to-

point measurements, numerous rig measurements were conducted. (For the rig measurements the location of the transmitter was fixed whereas the receiver was moved in a controlled direction in space.) The very common assumption used in cellular communications where radio links are subject to Rayleigh fading, which typically arises when a receiver is moving through a standing wave pattern with multiple scatterers in the vicinity, was confirmed by our numerous rig measurements from static environments in Iggesund [15]. However, our extensive sensor node-to-sensor node measurement campaigns, conducted at Iggesund and at two other process industries, confirm that static channels are rare, particularly when observing the radio environment over several minutes and hours, see [15], [16].

The typical situation in industrial environments, like the one in Iggesund, is that wireless channel variability in node-to-node links is caused by objects moving in the vicinity of, or in between, the sensor nodes. Examples of such a channel gain variability at the finish line of the paper mill and at the cooker environment are illustrated in Figure 6a and Figure 6b, respectively.

A closer look at Figure 6a reveals that the channel gain can vary with some 20-30 dBm and stay in a higher or lower dB region for several minutes and even hours. In Figure 6a the link variability is caused by a crane, located in the ceiling of the building, moving finished high quality paper from the roll up section to the floor and from one location on the floor to another where they are temporarily stored for later cutting and long term storage. In this case the intermediate storage of the paper rolls shadowed the radio link between the two nodes causing a significant change in the channel gain, see Figure 7a. In the time interval $[4.5 - 8.5]$ hours in Figure 6a the intermediate storage on the floor next to the roll up section was cleared and the channel gain increased for a period of several hours. A similar channel gain variability was observed at several other locations at the paper mill. However, at the starch cooker location, see Figure 7b, the channel gain variability was primarily caused by people moving in the narrow aisle close to the sensor node locations, see Figure 6b. Here the variability was in the range of 10-20 dBm. This indicates that a careful channel modelling is required, should energy efficient and low latency communications be attained, which constitute a prerequisite for low latency controller design.

Parameter estimation

When taking the variability of several links into account, Maximum Likelihood estimation of the model parameters reveals that neither Rayleigh or Rice, nor log-Normal distributions are solely adequate for describing the fading characteristics in a typical paper mill environment, see Figure 8. It is clear that the Nakagami-lognormal (Gamma-lognormal (GLN) in the power domain) compound distribution gives the best fit to the link measurement data acquired from the extensive measurement campaign conducted at the paper mill. Figure 8a depicts the estimated and

empirical cumulative power level distribution in dB whereas Figure 8b illustrates the theoretical and empirical average bit error rates (BER) for different distributions. Evidently, selecting the wrong fading distribution will have a detrimental effect on both energy expenditure and BER. In Figure 8, a one component compound distribution was considered. However, when performing a more in-depth identification based on the Iggesund measurement data over different time horizons, two fading components, (see "Radio Model Selection") are frequently required as is illustrated in Table 1. Measurement campaigns conducted at other industrial sites show that even three components might be required in some cases. From Table 1 we observe that for one hour segments one component suffices in 59% of the cases. In those one component cases, a GLN channel model fits the data best in 39% of the cases, whereas in 20% of the cases a G channel model is sufficient. In 34% of the total cases a two component compound model consisting of either G or GLN combinations turns out to be the best choice.

The situation is similar for four hour segments, but in this case a two component compound model is somewhat less frequent. For the sixteen hour segments, only in 15% of the cases a two component compound model was appropriate. We can thus conclude that in most cases a one component GLN model is a good description of the link variability at the Iggesund site. In other cases, such as for the Sandviken rolling mill measurement campaign, a two component model was the most appropriate choice for the 16 hour segments. These findings suggest that before a wireless control network is to be deployed at a new industrial site, a measurement campaign should be conducted to determine the required complexity of the fading distributions. Then both better BER and energy expenditure figures can be obtained.

Modeling joint behavior of radio channels in industrial environments

In this section, we extend the analysis of the radio channel measurements from the previous section and study the joint behavior of radio links. Specifically, by partitioning the link measurements into volatile and quiescent periods using hidden Markov models (HMM), we identify which links that are likely to experience severe fading simultaneously. The study is motivated by emerging routing protocols for wireless sensor networks (WSNs) where multipath diversity has been considered a key for achieving a timely data transfer [17].

These protocols transmit multiple copies of each data packet over parallel paths and this technique is most effective if transmission failures over the paths are uncorrelated. For instance, if a single event affects the quality of several paths, then there is little gain from the multipath diversity. In a scenario where a sensor node has multiple neighbors, from which a subset is to be selected as relaying nodes, the gain from the multipath diversity is increased if the selection process uses information on correlations in link quality among its neighbors. In this section we

outline an algorithm for detecting such correlations. We also demonstrate the performance of the algorithm on measurements of channel gains obtained from a network of nodes deployed in the vicinity of the previously mentioned starch cooker. The results show that it is common that some links undergo joint changes in link quality and we describe how this information could be incorporated into the design of multipath routing protocols.

Measurements

For the purpose of the analysis in this section, we focus on measurements obtained from seven wireless sensor nodes. These were deployed in the vicinity of the starch cooker and Figure 9 illustrates a map of the deployment area which included heavy machines and a large amount of metal objects.

In Figure 9, we picture a scenario where the node marked RX is a sensor node that is listening to transmissions from six of its neighbours that are all closer to the intended gateway, which is not depicted in the figure. The objective of the RX node is to select a subset of these neighbours as relaying nodes and, as will be described in more detail below, the subset should be selected so that the gain from the multipath diversity is increased.

The transmissions were performed in a round-robin fashion where each of the nodes with label 1-6 sent a packet to the RX node which recorded the received signal strength (RSS) of the incoming transmissions. Each node sent a packet every 0.125 seconds and measurements were conducted for three hours. A short segment of the resulting time series is illustrated in Figure 10.

As described in the previous section, the fading distribution of each link switched abruptly between volatile periods and more quiescent periods, where the channel gain could vary on the order of 20 dB in the former case. Moreover, initial studies of the measurements showed that, for each link, the volatile periods had a roughly similar spectrum. Hence, to detect changes in volatility of the monitored links, we propose a two state HMM where each state generates observations from an autoregressive (AR) process. For future reference, we let $\hat{z}_{l,t}$ denote the state of link l at time t, where $\hat{z}_{l,t} = 1$ indicates the volatile fading state and $\hat{z}_{l,t} = 0$ the quiescent fading state. In [18], Rabiner outlined an algorithm for inference of such models and we summarize the most important steps in "Data Generation Model". Finally, the inferred state sequence, which partitions each link into periods of volatile and quiescent behavior, will be used to identify links that are likely to experience severe fading simultaneously.

Results

Movement in the vicinity of the nodes mostly consisted of personnel that were walking along the paths that are marked by double dashed lines in Figure 9. Since the nodes were positioned in two clusters, where we for future reference let cluster 1 denote nodes 1-4 and cluster 2 denote nodes 5-6, passing personnel induced time varying shadow fading that often affected all the links in a cluster. However, due to the spatial separation between the clusters, it was unlikely that both of them were shadowed simultaneously.

In Figure 10, the background color indicates the estimated state sequence, $\hat{\mathbf{z}}_l$, from the HMMs. As expected, there is a tendency for the nodes in cluster 1 to have overlapping volatile regions. The same tendency can be observed for cluster 2. However, the volatile regions between nodes from different clusters show more sporadic overlap.

Table 2 lists the empirical probabilities, $o_{i,j}$, that $\mathbf{x}_j$ is in the volatile state given that $\mathbf{x}_i$ is in the volatile state, which can be computed as,

$$o_{i,j} = \frac{\sum_{t=1}^{T} \hat{z}_{i,t}\hat{z}_{j,t}}{\sum_{t=1}^{T} \hat{z}_{i,t}}. \tag{1}$$

The blue and red fields highlight the sparsity of the table which indicates that, for instance, if $\mathbf{x}_1$ is in the volatile state, then it is likely that $\mathbf{x}_2$, $\mathbf{x}_3$ and $\mathbf{x}_4$ are also in the volatile state. However, it is less likely that $\mathbf{x}_5$ or $\mathbf{x}_6$ is in the volatile state.

In summary, by using HMMs, a sensor node can identify correlations in link quality among its neighbours. This information can potentially be useful in a scenario where the node wants to transmit data to a sink node using a subset of these neighbours as relaying nodes. In this case the robust choice, in the sense that the selected paths drop packets independently, is to send the packet to the neighbors which exhibit no or weak correlation in link quality.

Energy harvesting in wireless networks

Employing many additional sensors to a large plant can have several significant advantages such as enabling more complex signal processing and control algorithms due to more information being available. Using wireless sensors and appropriate routing protocols as described above already simplifies this process by avoiding wires for information flow. Flexibility when adding wireless sensors to the plant can further be enhanced if the sensors do not have to be connected to the electricity grid but instead are powered using energy harvesting. For instance, at the starch cooker at Iggesund paper mill, several energy sources such as hot pipes or tanks, rotating or vibrating parts or the lighting can be used to extract energy to power wireless sensors.

In order to study the energy harvesting capabilities at Iggesund paper mill, several wireless energy harvesting sensors were employed. Some sensors, such as the one shown in Figure 11a were equipped with small solar cells to harvest energy from the lighting. Since some mixing tanks and pipes get very hot, the resulting large temperature gradients can be used to harvest energies using Peltier elements such as shown in Figure 11b. The harvested energy was stored in a local rechargeable battery to be used for data transmission immediately or at a later stage.

Then, a simple algorithm was used to control the sensors: measurements should be submitted every 1 to 3 seconds if sufficient energy is available in the sensor's battery or, otherwise, as soon as enough energy is available again. Figure 12 shows the time between consecutive packets received from a wireless sensor located close to node 4 in Figure 9 for a measurement campaign over several hours. Here, the harvested energy apparently varies periodically since the pipe delivers a product of a reoccurring batch process, of slightly more than one hour length. Since the energy is harvested from a hot pipe, the amount of harvested energy significantly depends on the temperature of the pipe, which varies periodically due to the batch process. Thus, when the pipe cools down after the necessary amount of hot liquid has been delivered for the current batch, less energy can be harvested and the time between sent packets increases as observed in Figure 12. Large time gaps between consecutive packets, and long periods of time where no packets can be sent due to a lack of harvested energy, are highly undesirable in practical settings. One method to improve this situation is to derive better algorithms to allocate the available harvested energy. As for the energy harvesting scenario illustrated in Figure 12, information or a model of the underlying batch process should be used to predict and plan for the available harvested energy over time so that, for instance, the maximal time between consecutive packets is minimized.

To model the available energy over time, first denote the harvested energy at sensor m and time slot k by $H_m(k)$. Several methods exist to model the harvested energy such as Markov chains, motivated by empirical measurements reported in [19]. For instance, for the harvesting process underlying in Figure 12, additional information such as the temperature of the liquid in the pipe can be used to derive more accurate models. The energy harvested at time slot k is stored in the battery, and can be used for different tasks such as data transmission in the $k+1$-th time slot. Hence, the dynamics of the battery level of sensor m at time $k+1$ can be described by $B_m(k)$, evolving according to

$$B_m(k+1) = \min\left\{B_m(k) + H_m(k) - E_m(k); \quad \hat{B}_m\right\}, \tag{2}$$

where $E_m(k)$ denotes the energy used by sensor m at time k and $\hat{B}_m$ denotes the battery capacity.

This battery model, together with a model for the harvesting process, can then be used to

derive suitable energy allocation policies. For instance, if the harvesting sensor should transmit data over a fading channel, an optimal energy allocation policy could be derived, that chooses suitable transmission energies depending on the battery level and the channel gain in order to maximize a desired quantity of interest.

Event-based control

In event-based networked control systems sensors transmit only when certain conditions are satisfied. Such systems have been quite widely studied over the last couple of decades, mainly motivated by their lower requirements on communication compared to conventional periodic control, see "Advances in Event-based Control". In this section, we discuss the event-based control of the starch cooker process with wireless sensors, as illustrated in Figure 5. Especially, we describe how event-based feedback and feedforward control could be implemented for that process.

Let us focus on one specific control loop of the starch cooker, namely, the fine water flow control. The fine water flow is controlled by using sensor S_5 and actuator A_5 in Figure 5 to obtain the desired final starch paste solution. The concentration is possibly disturbed by the change of the steam flow into the steam ejector, or the change of the starch concentration after the screen. Since such a disturbance only slowly affects the final product, it is difficult to mitigate the influence effectively by feedback control. Feedforward compensation is able to adjust the fine water flow rate as soon as the disturbance is detected. To do this, the steam flow and the opening of the steam valve are monitored by the sensor S_4 and the actuator signal A_4, respectively. Since disturbances act only now and then, it is reasonable to use event-based compensation, that is, to let S_4 and A_4 transmit their sensor and actuator values only when each value changes more than a certain threshold. We illustrate the merit of such an event-based feedforward compensation scheme in this section as well as the event-based feedback control. To mimic a control loop in the starch cooker, let us introduce a continuous-time linear system given by

$$\dot{x}_p(t) = Ax_p(t) + Bu(t) + \tilde{B}w(t) \tag{3}$$

$$y(t) = Cx_p(t) \tag{4}$$

where x_p is the plant state, y the plant sensor output, w the disturbance, and u the control input to the plant. The disturbance w affects the plant through the disturbance dynamics

$$\dot{w}(t) = A_d w(t) + B_d d(t) \tag{5}$$

where d is the external disturbance which can be measured by the disturbance sensor $y_d(t) = C_d d(t)$. For this system, a PI control with discrete sampling is implemented as

$$\dot{x}_c(t) = y(t_k) - r(t)$$
$$u(t) = K_p(y(t_k) - r(t)) + K_i x_c(t) + K_f y_d(t_\ell)$$

where x_c is the integrator state, r the reference (setpoint) signal, and t_k the time of sample k of the event generator of the plant sensor, t_ℓ the time of sample ℓ of the disturbance sensor. Furthermore, K_p and K_i are appropriately tuned proportional and integral gains, respectively. The feedforward gain is denoted K_f. The block diagram of the event-based control system is depicted in Figure 13.

Let us first consider the event-based feedforward control, corresponding to that the event generator in the feedback loop of Figure 13 is periodic. A disturbance event is generated at the sensor when the condition $|y_d(t) - y_d(t_\ell)| \geq \bar{e}_d$ is satisfied, where t_ℓ is the last measurement instance and $\bar{e}_d$ some prespecified event threshold.

Figure 14 shows three simulations of disturbance responses for a first-order system with and without feedforward control, and with PI feedback control in all three cases. Note that we consider periodic samplings of the feedback control loop in all cases. The upper plot shows the disturbance, the middle plot the plant state, and the lower plot the PI control signal. We note that even if the feedforward event generator only transmits nine measurements of the disturbance (red circles in the upper plot), it performs equally well to the continuous-time feedforward control (green). Further discussion on the design of feedforward event-based control is given in [20].

Now instead consider the case when there are no disturbance: $d(t) \equiv 0$ for all $t \geq 0$. Then the system in Figure 13 is a conventional event-based PI control system studied by many authors in the literature [21]–[27]. Some of these works [23], [24], [26] investigate event-based PI control with events generated when the measurement error reaches above a threshold $\bar{e}$:

$$|y(t) - y(t_k)| \geq \bar{e}.$$

In the thesis [23] and the subsequent paper [24], the performance of PI control with this sampling scheme was evaluated in some industrial control loops at the Iggesund Paperboard. It was demonstrated that with a careful selection of the threshold the sampling may be reduced as much as 90% or more with only a marginal loss of control performance. Figure 15 (which is re-drawn from Figure 3 in [24]) shows step responses for a reject tank.

In Table 3, the results are summarized for three performance measures: integrated absolute control error *IAE*, integrated squared control error *ISE* and average overshoot for the negative

and positive steps. The table also gives the communication reduction in percent relative to fast periodic control. More advanced set-point tracking for event-based PI control were developed in [27] modifying the event-based PIDPLUS [28].

An interesting topic for further study is the combination of event-based sampling for the various sensors in other control architectures, not only feedback and feedforward configurations.

Proof-of-concept implementation at Iggesund Paperboard

In this section we will present a proof-of-concept implementation at Iggesund Paperboard in the process section introduced in Section IV. The part of the starch cooking section that was used for the field-trials, is illustrated in Figure 16. The starch is produced in batches. A batch is started when the level of the storage tank reaches a predefined low threshold value and stopped when the level of the storage tank reaches the high threshold value. During the week when we controlled the starch cooking process, the production rate was set to 1500 kg/h. A typical batch was running for approximately one hour and then it was stopped for 2-3 hours depending on the quality of the paperboard produced.

A separate process controller was installed in parallel with the existing control system to have a fall back solution, should any failures during the experiments arise. The control loops were closed using both wireless sensors (S_4, S_5, S_6) and wireless actuators (A_4, A_5, A_6), see Figure 16. The control loops were implemented in the ABB AC800M controller using standard PID controllers with the same control parameters as in the existing control system.

Furthermore, the wireless system was equipped with a deterministic failure detection feature, and therefore, the additional process controller would be able to signal to the normal control system to take over in case of a detected error. The wireless actuators would also detect such an error at the same time as any of the other communication peers in the system, thus being able to electrically switch back the control of the valves to the normal control system. It might seem to be ambitious to implement such functionality to conduct experiments for research, but it was required for us to conduct measurements and control 24 hours a day for five calendar days without having researchers stand-by all the time to manually restore production in case of a failure.

The additional process controller, AC800M from ABB, was connected to a gateway in the process via Profinet IO, utilizing an existing fiber between the process and the marshalling room where the control equipment was installed. In the process, we installed the wireless instruments and the wireless actuators and connected them to the existing valves and instrumentation using 4-20mA interfaces. The gateway and the field devices were realized by assembling two off-the-

shelf evaluation boards in an IP67 enclosure as shown in Figure 17.

Challenges with existing industrial wireless sensor network standards such as WirelessHART or ISA100 for wireless control has previously been identified [29]. Therefore solutions to overcome limitations such as, for example, real-time up-links, seamless recovery in case of link failures, as well as diagnostics to take the end-nodes into a safe state in a timely manner in case of communication errors, has been proposed and implemented. One such solution is Realflow [30] that has been used in this proof-of-concept implementation, as well as a new time synchronization protocol [31] to have more precise Time Division Media Access. In addition, solutions to enable several concurrent data flows with different priorities have been implemented to have a deterministic communication network supporting on-line changes and topology changes without any deadline misses in the real-time communication paths, which is required for control applications.

Consider the flow control depicted in Figure 18. In the beginning of the batch sequence, just before 21:00, the flow controller is enabled to keep a water flow of 41 liters/minute. At this moment the control valve of the pressure controller is opened to 50% to flush out remainders of starch from the previous batch as can be seen in Figure 19. In parallel with starting the heating of the boiler the pressure controller is enabled to maintain a pressure of 3.3 Bar in the boiler. After that the batch sequence enables a ramp in the output of the control valve to heat the boiler with steam. When the temperature of the boiler is close to its set-point of 138 degrees Celsius the temperature controller is enabled to maintain the temperature. This can be seen in Figure 20, the knee on the yellow line some minutes after 21:00.

Just before 22:10 the level of the storage tank have reached the upper threshold and the control valves to the storage tanks are closed and a cleaning process starts. In Figure 18, a flow disturbance is noticed when the pressure valve is opened for cleaning (see Figure 19). The cleaning process finished at 22:15 and the starch cooking system is ready for another batch when the storage tank level is reaching its lower threshold.

The batch sequence was started approximately every third hour during the five day experiment period. During this period the plant operators could neither identify any significant differences between the wireless- and Profibus controlled process, nor did the production system detect any deviations with respect to the control limits installed to provide early warning that the process section would be in need of maintenance. In addition, the safety functionality that would restore operation to the normal production system was never invoked, since there were no three consecutive communication errors during five day period. Even when comparing production data between the wireless- and normally controlled process, no differences could be discerned.

However, one could observe slightly different variations in the final concentration of the starch. We were told by the operators that they could see such variations every now and then in the normal production system, and the variations were explained by variations in the density of the ingredients in the storage tank before mixing. This implies that the feeders' duty cycle will feed a small variation in volume of the ingredients, which varies over time depending on how full the tank is.

All in all, the general conclusion by the operators and the automation engineers was that they could not tell if the process was controlled with a wireless- or wired technology. Due to the inherent variations in the quality of the process ingredients we cannot quantify the difference in control performance between the wireless and Profibus controlled process. However, our experiments indicate that it is indeed feasible to design and implement wireless systems for process control and there is no need to treat them differently than the wired control counterparts, neither from a quality, nor from a control performance perspective. Furthermore, our wireless control experiment indicates that it is indeed feasible to use wireless control for continuous operation and production. From an availability perspective this is however a too short a time to draw any general conclusions, but comparing the performance indicators from the wireless installation with the same performance indicators using the Profibus network suggests that it would be possible to reach the desired availability with a wireless installation.

Conclusions

In this paper we have addressed important research problems that are critical to solve before deploying wireless control systems in the process industry. In large industrial plants such as, for example, a paper mill, information from thousands of sensors would then have to be handled swiftly over wireless links. We have addressed the importance of having a correct characterization of the radio environment, the use of suitable network protocols for routing sensor information to the gateways, efficient use of harvested energy from the environment, as well as the use of robust, possibly event based, and reconfigurable control algorithms. Furthermore, we have deployed a wireless networked control system addressing these aspects at the Iggesund Paperboard papermill. Long term tests were conducted on one of the mill's starch cookers during normal production over five consecutive days. The tests were very successful and the operators could not distinguish the wireless control system from the wired, which suggests that it is indeed possible to replace wired control systems with wireless, even in a complex industrial environment.

Acknowledgements

This work was supported by VINNOVA, The Swedish Governmental Agency for Innovation Systems. Many people have contributed to the results underlying this work. In particular we would like to mention Piyush Agrawal, Subhrakanti Dey, Mikael Gidlund, Ewa Hansen, Jonas Neander, Tommy Norgren, Tomas Olofsson, Jonathan Styrud and Junfeng Wu.

The authors are grateful to Iggesund Paperboard for letting us conduct radio channel measurements and wireless control tests on the paper mill's starch cooker during normal production.

References

[1] T. S. Rappaport and C. D. McGillem, "UHF fading in factories," *IEEE J. Sel. Areas Commun.*, vol. 7, no. 1, pp. 40–48, 1989.

[2] A. Willig, "Recent and emerging topics in wireless industrial communication," *IEEE Trans. Ind. Informat.*, vol. 4, no. 2, pp. 102—124, 2008.

[3] P. Antsaklis and J. Baillieul, "Special issue on technology of networked control systems," *Proc. IEEE*, vol. 95, no. 1, pp. 5–8, 2007.

[4] J. P. Hespanha, P. Naghshtabrizi, and Y. Xu, "A survey of recent results in networked control systems," *Proc. IEEE*, vol. 95, no. 1, pp. 138–162, 2007.

[5] P. Park, S. Coleri Ergen, C. Fischione, C. Lu, and K. H. Johansson, "Wireless network design for control systems: a survey," *IEEE Commun. Surv. Tutor.*, vol. 20, no. 2, pp. 978–1013, 2018.

[6] H. Forbes, "ExxonMobil's quest for the future of process automation," *ARC Insights, ARC Advisory Group*, 2016.

[7] D. Clark, "The IoT of automation - a totally new way to look at control and automation in the process industries," in *Proc. LCCC Workshop Process Control*. Department of Automatic Control, Lund Institute of Technology, Lund University, 2016.

[8] I. F. Akyildiz, W. Su, Y. Sankarasubramaniam, and E. Cayirci, "Wireless sensor networks: a survey," *Computer Networks*, vol. 38, no. 4, pp. 393–422, 2002.

[9] V. C. Gungor and G. P. Hancke, "Industrial wireless sensor networks: Challenges, design principles, and technical approaches." *IEEE Trans. Ind. Electron.*, vol. 56, no. 10, pp. 4258–4265, 2009.

[10] T. S. Rappaport, *Wireless communication: Principles and Practice*, 2nd ed. Prentice Hall PTR, New Jersey, 1996.

[11] H. Hashemi, M. McGuire, T. Vlasschaert, and D. Tholl, "Measurements and modeling of temporal variations of the indoor radio propagation channel," *IEEE Trans. Veh. Technol.*, vol. 43, no. 3, pp. 733–737, 1994.

[12] T. S. Rappaport, "Characterization of uhf multipath radio channels in factory buildings," *IEEE Trans. Antennas Propag.*, vol. 37, no. 8, pp. 1058–1069, 1989.

[13] H. Hashemi, "The indoor radio propagation channel," *Proc. IEEE*, vol. 81, no. 7, pp. 943–968, July 1993.

[14] R. Bultitude, "Measurement, characterization and modeling of indoor 800/900 MHz radio channels for digital communications," *IEEE Commun. Mag.*, vol. 25, no. 6, pp. 5–12, 1987.

[15] P. Agrawal, A. Ahlén, T. Olofsson, and M. Gidlund, "Long term channel characterization for energy efficient transmission in industrial environments," *IEEE Trans. Commun.*, vol. 62, no. 8, pp. 3004–3014, 2014.

[16] T. Olofsson, A. Ahlén, and M. Gidlund, "Modeling of the fading statistics of wireless sensor network channels in industrial environments," *IEEE Trans. Signal Process.*, vol. 64, no. 12, pp. 3021–3034, 2016.

[17] M. Masdari and M. Tanabi, "Multipath routing protocols in wireless sensor networks: A survey and analysis," *Int. J. Future Gen. Comm. Netw.*, vol. 6, no. 6, pp. 181–192, 2013.

[18] L. Rabiner, "A tutorial on hidden markov models and selected applications in speech recognition," *Proc. IEEE*, vol. 77, no. 2, pp. 257–286, Feb 1989.

[19] C. K. Ho, P. D. Khoa, and P. C. Ming, "Markovian models for harvested energy in wireless communications," in *Proc. IEEE Int. Conf. Communication Systems*, 2010.

[20] T. Iwaki, J. Wu, and K. H. Johansson, "Event-triggered feedforward control subject to actuator saturation for disturbance compensation," in *Proc. European Control Conf.*, 2018, pp. 501–506.

[21] K.-E. Årzén, "A simple event-based PID controller," in *Proc. IFAC World Congr.*, vol. 18, 1999, pp. 423–428.

[22] M. Rabi and K. H. Johansson, "Event-triggered strategies for industrial control over wireless networks," in *Proc. Int. Conf. Wireless Internet*, 2008, pp. 1–7.

[23] T. Norgren and J. Styrud, "Non-periodic sampling schemes for control applications," Master's thesis, Uppsala University, 2011.

[24] T. Norgren, J. Styrud, A. J. Isaksson, J. Åkerberg, and T. Lindh, "Industrial evaluation of process control using non-periodic sampling," in *Proc. IEEE Conf. Emerging Technologies and Factory Automation*, 2012, pp. 1–8.

[25] C.-F. Lindberg and A. J. Isaksson, "Comparison of different sampling schemes for wireless control subject to packet losses," in *Proc. Int. Conf. Event-based Control, Communication, and Signal Processing*, 2015, pp. 1–8.

[26] G. A. Kiener, D. Lehmann, and K. H. Johansson, "Actuator saturation and anti-windup compensation in event-triggered control," *Discrete Event Dynamic Systems*, vol. 24, no. 2, pp. 173–197, 2014.

[27] U. Tiberi, J. Araújo, and K. H. Johansson, "On event-based PI control of first-order processes," in *Proc. IFAC Conf. Advances in PID Control*, 2012, pp. 448–453.

[28] T. Blevins, D. Chen, M. Nixon, and W. Wojsznis, *Wireless Control Foundation: Continuous and Discrete Control for the Process Industry*. International Society of Automation, 2015.

[29] J. Åkerberg, M. Gidlund, and M. Björkman, "Future research challenges in wireless sensor and actuator networks targeting industrial automation," in *Proc. IEEE Int. Conf. Industrial Informatics*, 2011, pp. 410–415.

[30] K. Yu, Z. Pang, M. Gidlund, J. Åkerberg, and M. Björkman, "Realflow: Reliable real-time flooding-based routing protocol for industrial wireless sensor networks," *Int. J. Distrib. Sens. N.*, vol. 10, no. 7, p. 936379, 2014.

[31] T. Lennvall, J. Åkerberg, E. Hansen, and K. Yu, "A new wireless sensor network TDMA timing synchronization protocol," in *Proc. IEEE Int. Conf. Industrial Informatics*, 2016, pp. 606–611.

TABLE 1. Obtained number of mixture components (Comp) in % after ML-optimization over one hour (1H), four hour (4H), and sixteen hour (16H) time segments acquired at Iggesund Paperboard in Sweden. Models identified and validated based on received signal strength (RSS) power measurements were, (see, "Radio Model Selection"): Gamma (G) and/or gamma – lognormal (GLN) compound models. (L) is lost packets, that is, packets where received signal strength (RSS) data could not be retrieved. Total number of time segments: 92 (46) for 1H and 4H (16H).

Segment	1 Comp		2 Comp			L
	G	GLN	G–G	G–GLN	GLN–GLN	
1H	20	39	13	14	7	7
4H	23	36	11	10	6	14
16H	30	42	7	4	4	13

TABLE 2. Empirical probabilities computed using (1) where $o_{i,j}$ is the element in the ith row and the jth column. The background colors highlight the block diagonal structure of the matrix which implies that the nodes belong to two distinct groups, where the nodes within the same group often were in the same fading state.

%	$\mathbf{x}_1$	$\mathbf{x}_2$	$\mathbf{x}_3$	$\mathbf{x}_4$	$\mathbf{x}_5$	$\mathbf{x}_6$
$\mathbf{x}_1$	·	0.74	0.90	0.79	0.17	0.14
$\mathbf{x}_2$	0.96	·	0.96	0.95	0.16	0.14
$\mathbf{x}_3$	0.67	0.55	·	0.75	0.16	0.14
$\mathbf{x}_4$	0.75	0.68	0.95	·	0.15	0.12
$\mathbf{x}_5$	0.23	0.17	0.29	0.22	·	0.7
$\mathbf{x}_6$	0.28	0.21	0.3	0.25	0.99	·

TABLE 3. Step response performances of three sampling schemes for the reject tank: Fast periodic $h = 0.5$ [s] (FP), slow periodic $h = 5$ [s] (SP), and event-based $\bar{e} = 0.5$ (EB). Performance is evaluated through communication reduction (CR) and the three measures integrated absolute control error (IAE), integrated squared control error (ISE), and over-shoot (OS).

Scheme	**CR**	$\int \lvert e(t) \rvert$	$\int \lvert e(t) \rvert^2$	**OS**
FP	0%	141.3	295.9	15.0%
SP	90.0%	229.7	486.2	53.7%
EB	87.9%	174.9	392.1	22.5%

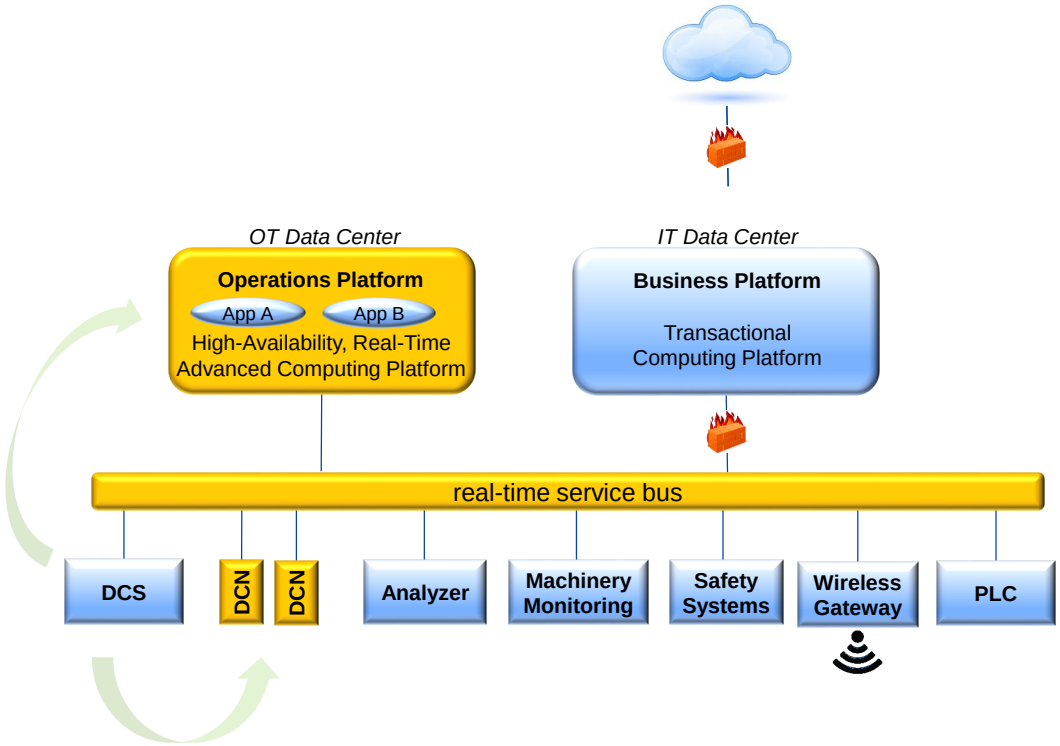

1

Figure 1. Layout of a future control architecture (with ExxonMobil's permission): The system contains distributed control nodes, used as dedicated single-channel I/O modules, with control capability. Through a real-time data service bus, they are connected to the operations open platform running open-source software. This setup together with a common "app" platform is expected to replace the traditional automation pyramid, which structurally separates process control, scheduling and planning to their own hierarchical levels; leading to a more flexible and cost effective paradigm.

Figure 2. The Iggesund paper mill, which is part of Holmen group, is in Iggesund. The small community in Iggesund is located on the coast of the Bothnian Sea, Sweden's east coast. The mill produces one of the world's leading paperboard brand, Invercote. About 700 people work in Iggesund paper mill and the factory produces about 420,000 tons of pulp and about 330,000 tons of cardboard every year.

Figure 3. Iggesund's paper mill has two paper machines of the kind mentioned above. The machines are 300 m long and produce state-of-the-art cardboard. The photo is taken from the wet end of the cardboard machine 2. At the far right of the picture is the wire section where the pulp comes out of the headboxes and is dewatered on the wire. The pulp then contains more than 99% water. To the left of the picture you see the drying unit where the cardboard is dried by steam.

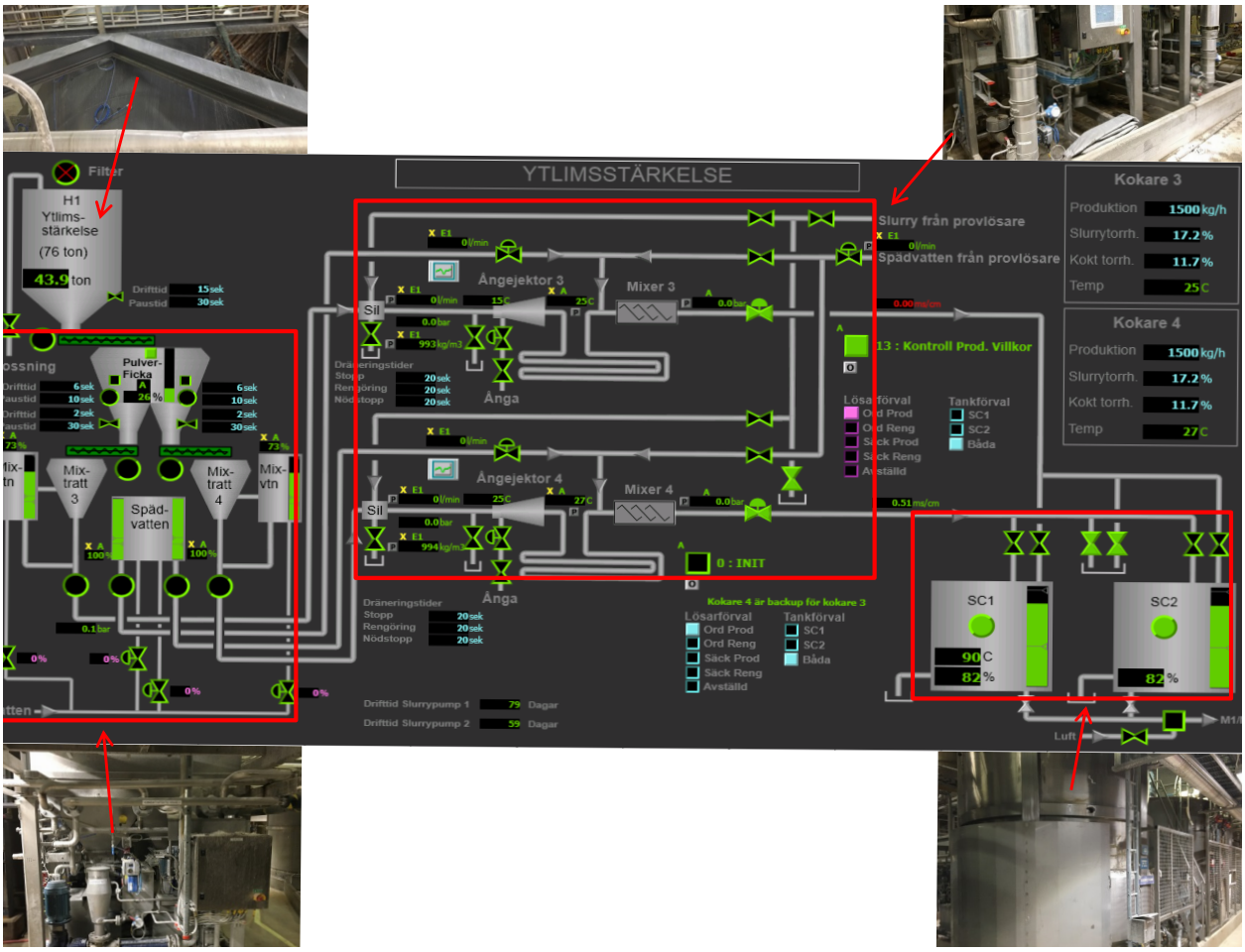

Figure 4. The starch cooker process illustrated by the operator panel in the middle and photos of the real process equipment in the corners above and below the operator panel. Top left: Starch powder buffer. Top right: Starch boiler. Bottom left: Mixing tank for starch powder and water. Bottom right: Storage tank for boiled starch. The red arrows relate the respective process equipment to the operator panel.

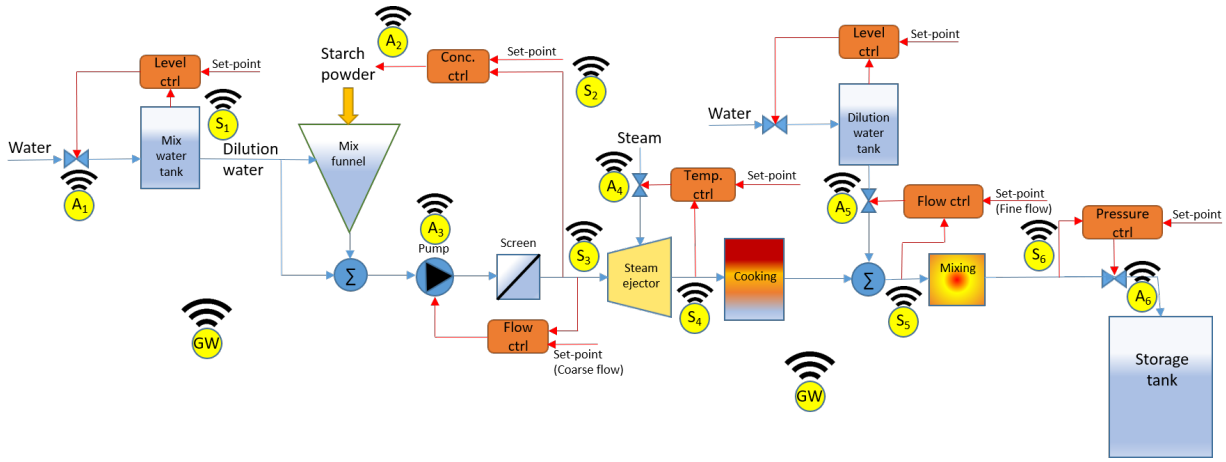

Figure 5. Block diagram of the Iggesund Paperboard starch cooker, also illustrated in the operators panel of Figure 4. The process starts with filling a water tank (depicted at the top left of the figure), from which water is used to mix with the starch in a mixing funnel. In order to remove lumps of starch, the mixture is pumped through a screen before steam is injected for cooking. In order to finely adjust the starch concentration after cooking, small amounts of dilution water might be added before storing the product in a storage tank (see the bottom right corner of the figure). The architecture, consists of multiple wireless feedback loops involving sensors (S_j) and actuators (A_j) to control each step of the process.

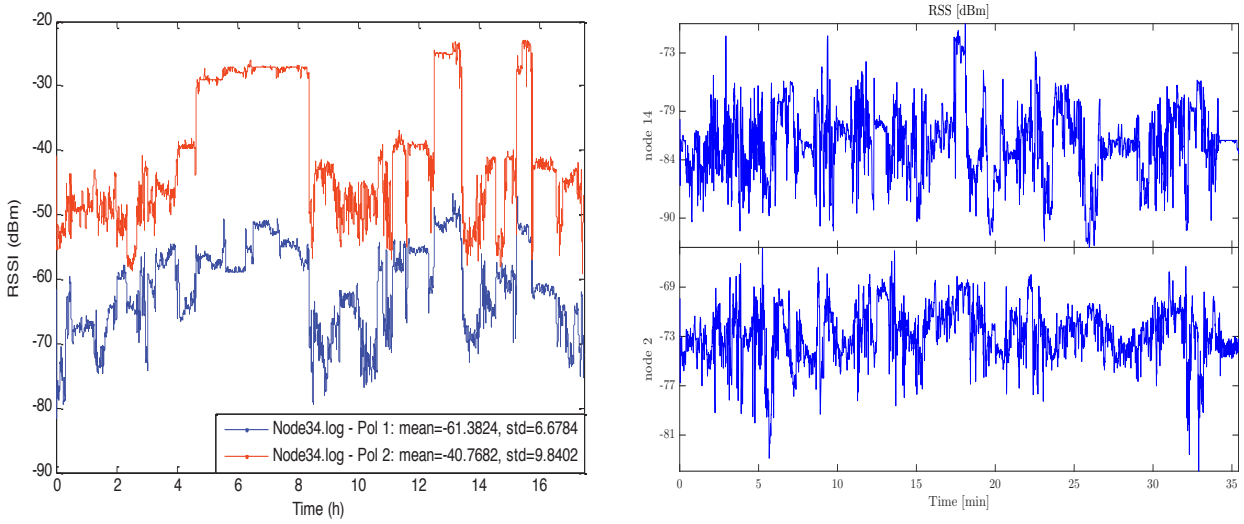

(a) (b)

Figure 6. Channel gain variability between two sensor nodes located next to the paper machine finish line at Iggesund Paperboard paper mill. The crane in the ceiling moving around the paper rolls causes the gain variability, (a) vertical polarization (red), horizontal polarization (blue), and channel gain variability realizations between two pairs of sensor nodes in the starch cooker section. The variability is primarily caused by people moving in the environment of the sensor nodes, (b).

(a) (b)

Figure 7. Iggesund Paperboard paper mill. (a) Channel measurement between two nodes located on opposite sides of the aisle next to the paper mill finish line in Iggesund. A typical channel gain variability is depicted in Figure 6 a. The green dots indicate the approximate positions of the sensor nodes. (b) Aisle in the cooker environment where wireless sensor nodes were deployed. Typical channel gain variabilities between pairs of nodes are depicted in Figure 6 b.

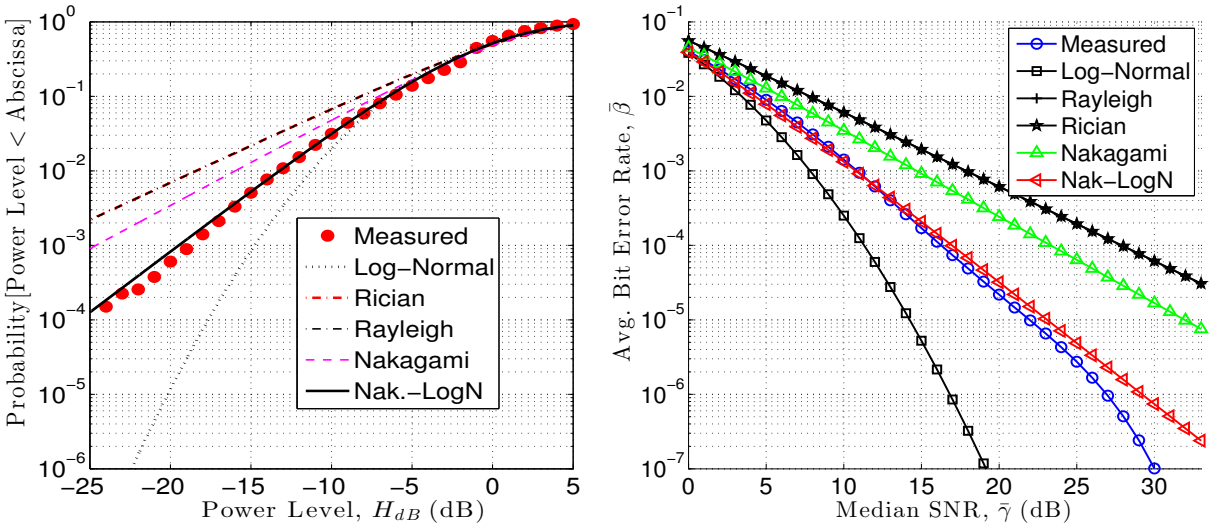

(a) Estimated and empirical cumulative power level distributions (in dB) based on all measured links over 17 hours.

(b) Theoretical and empirical average bit error rate (BER) as a function of the median signal to noise ration (SNR) based on all measured links over 17 hours.

Figure 8. Theoretical and empirical evaluations taken over all wireless link data acquired during a measurement campaign at Iggesund Paperboard, Sweden during 17 hours. The diagrams above are from [15] and republished here with the consent of IEEE.

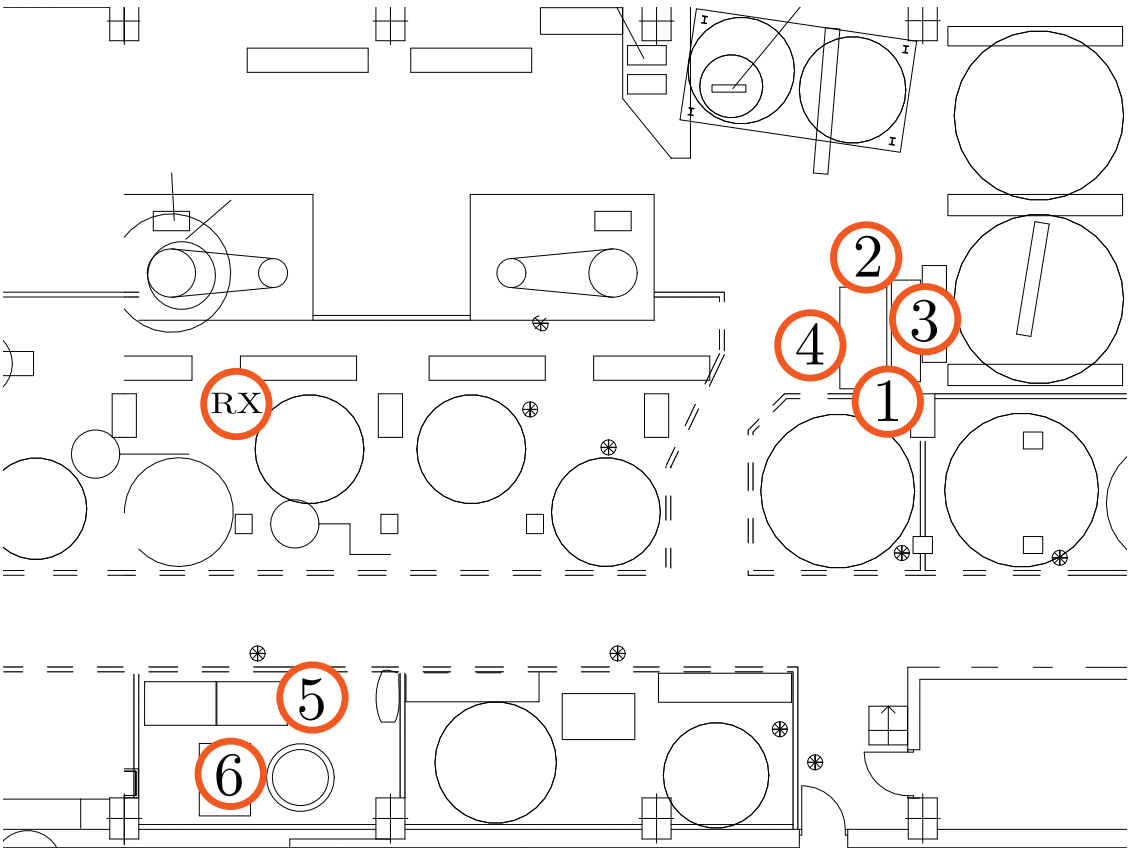

Figure 9. Overview of the deployment area at the paper mill in Iggesund. The circles indicate the positions of the wireless sensor nodes which were deployed in close proximity to machines to mimic a realistic wireless control scenario.

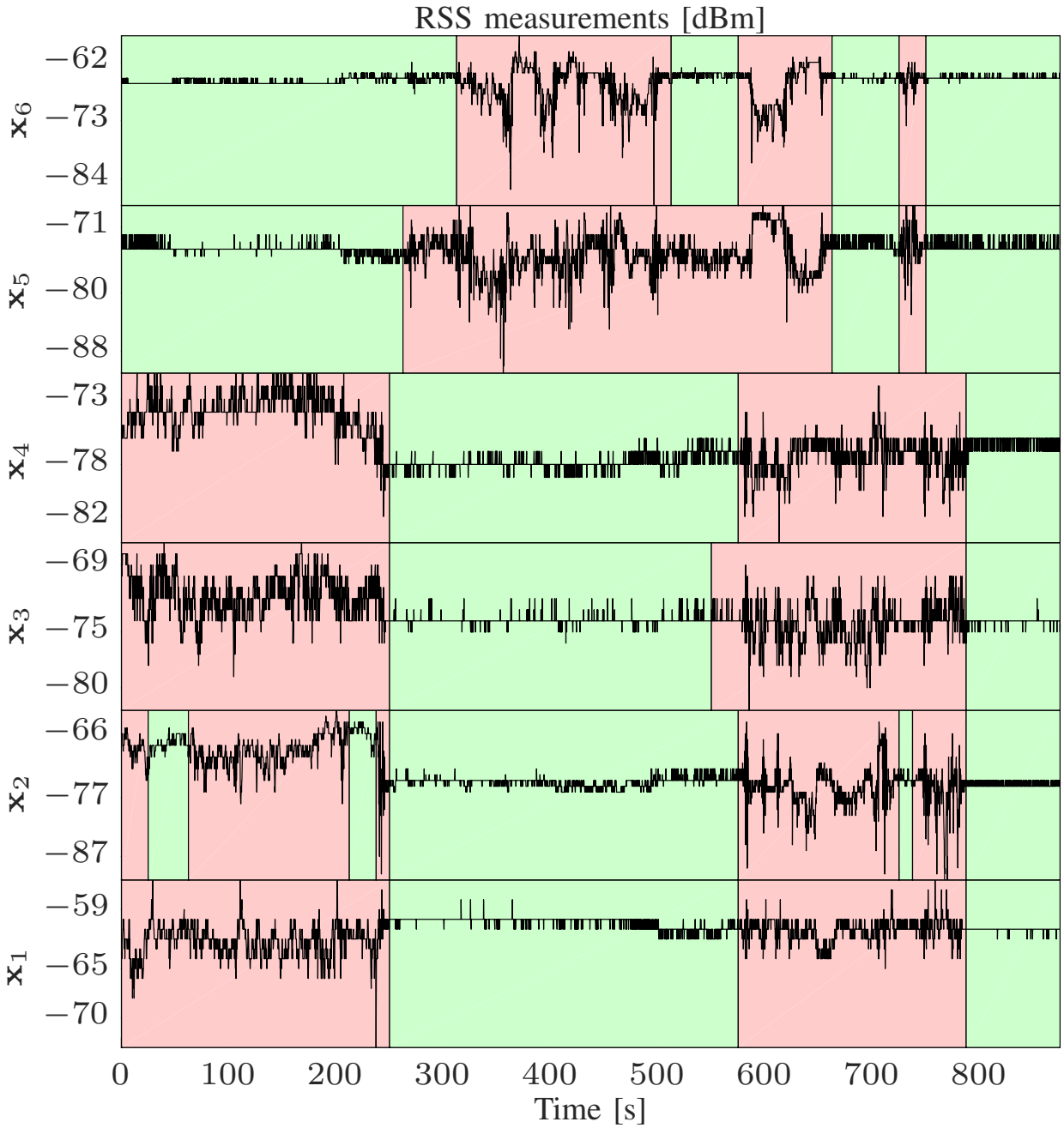

Figure 10. Time series of recorded received signal strength (RSS) for the network in Figure 9. The green and red fields mark the estimated periods of quiescent and volatile fading, that is, where $\hat{z}_{l,t} = 0$ and $\hat{z}_{l,t} = 1$, respectively. Since the nodes $\mathbf{x}_1$-$\mathbf{x}_4$ were positioned relatively close to each other, we see that they often were in the same fading state. As expected, nodes $\mathbf{x}_5$ and $\mathbf{x}_6$ exhibited similar behavior.

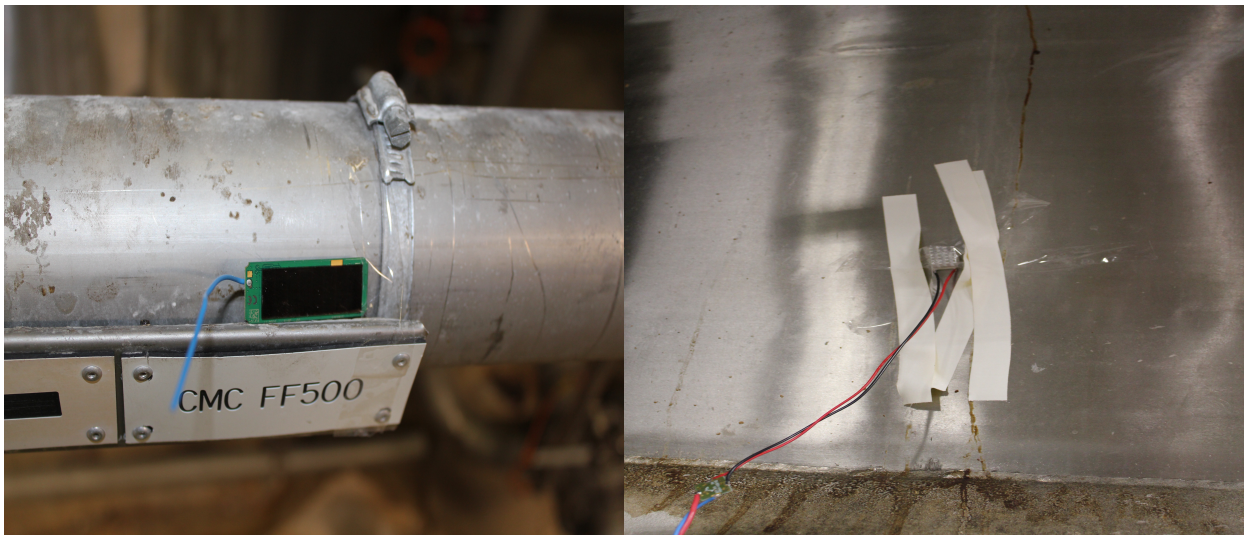

(a) Wireless sensor, powered by solar cell. (b) Peltier element at hot tank.

Figure 11. Energy harvesting devices used for experiments at Iggesund paper mill. (a) Small wireless sensors with solar cells where used to harvest energy from the factory lighting. (b) Also, Peltier elements were located at several hot surfaces (for example pipes and tanks) to harvest energy from the temperature gradient.

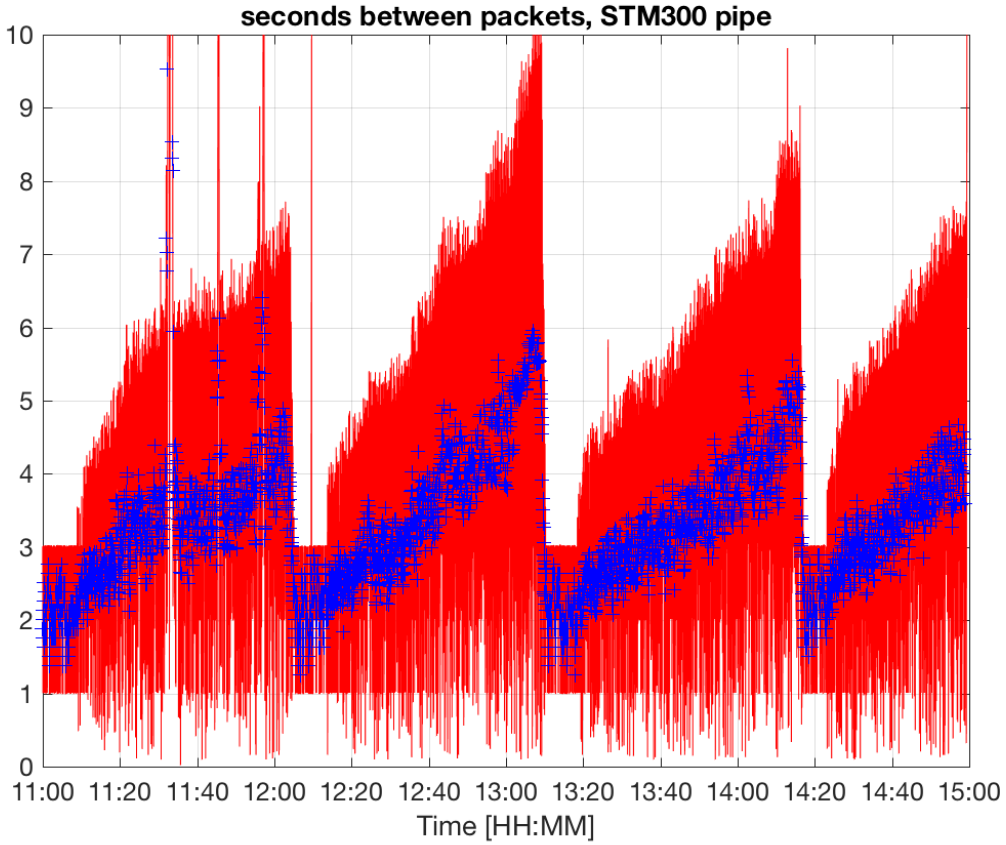

Figure 12. Time between consecutive packets received from a wireless sensor at node 4 powered by a Peltier element attached to a hot pipe; raw data (red) and filtered (blue). It is clearly visible, that the time between two consecutive packets changes periodically. This is due to the harvested energy that is used to send the packets also changes periodically. Indeed, the pipe, at which the Peltier element was located, transports hot liquids to a batch process. This takes a few minutes, in which the pipe gets very hot. Afterwards, the temperature decreases slowly, so that the harvested energy also slowly decreases and the time between the packets increases. The batch process is then repeated roughly every hour so that the patterns repeat periodically.

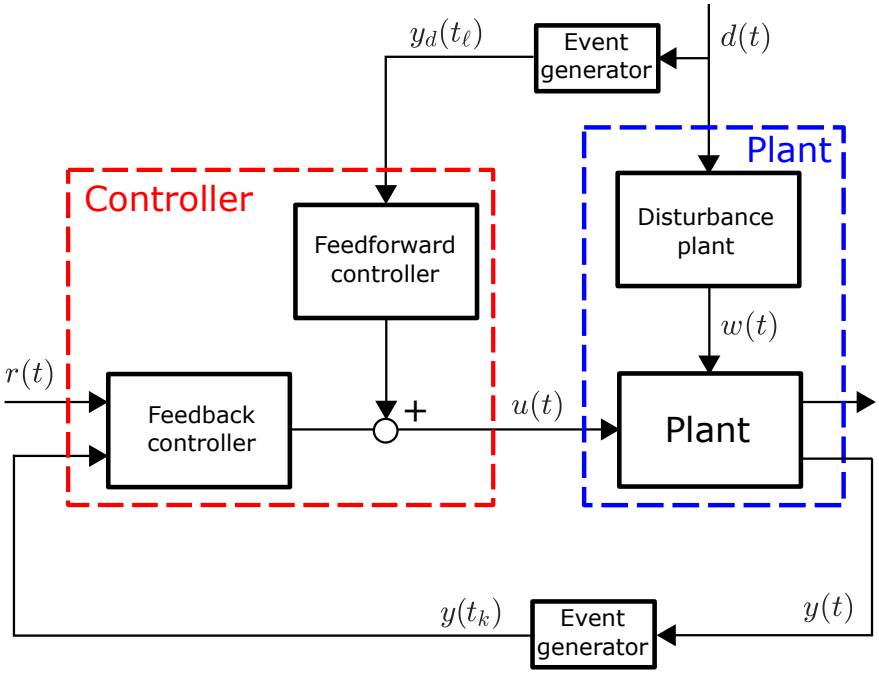

Figure 13. Block diagram of event-based feedback and feedforward control. The red box indicates the controller. The feedforward controller adjusts the control signal from the feedback controller based on the information from the disturbance sensor. The blue box indicates the plant which consists of the disturbance plant and main plant. Event generators are introduced at the plant and disturbance sensors. Transmission events are generated if the sensor measurements change significantly.

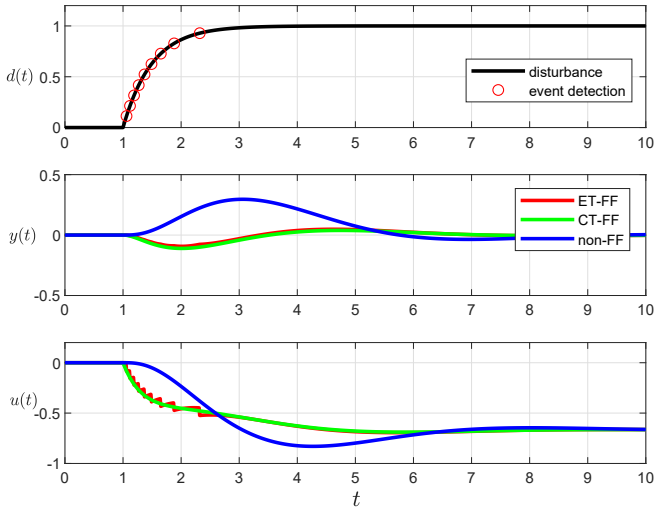

Figure 14. Simulations of disturbance responses. Top: Disturbance and event generation times. Middle: Outputs of three cases; (i) with event-based feedforward control (red, ET-FF), (ii) with continuous-time feedforward control (green, CT-FF), and (iii) no feedforward control (blue, no-FF). Bottom: Inputs of the same three cases. The simulations show that the event-based feedforward control performs equally well to the continuous-time feedforward control with only nine transmissions of the disturbance measurements. See [20] for more details.

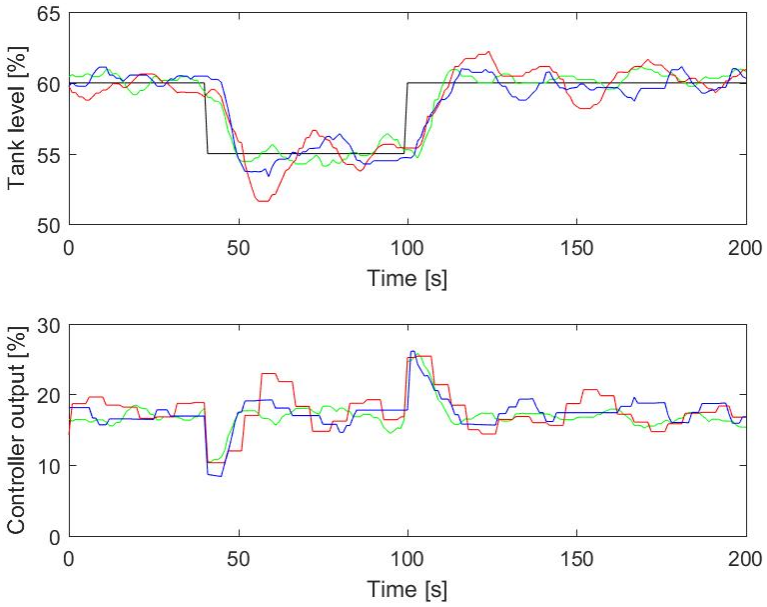

Figure 15. Step responses on the reject tank process at Iggesund for three sampling schemes: Fast periodic $h = 0.5$ [s] (green), slow periodic, $h = 5$ [s] (red), event-based $\bar{e} = 0.5$[s] (blue) control. The event-based control still has similar performance compared to fast periodic despite almost 90% communication reduction. See also Table 3.

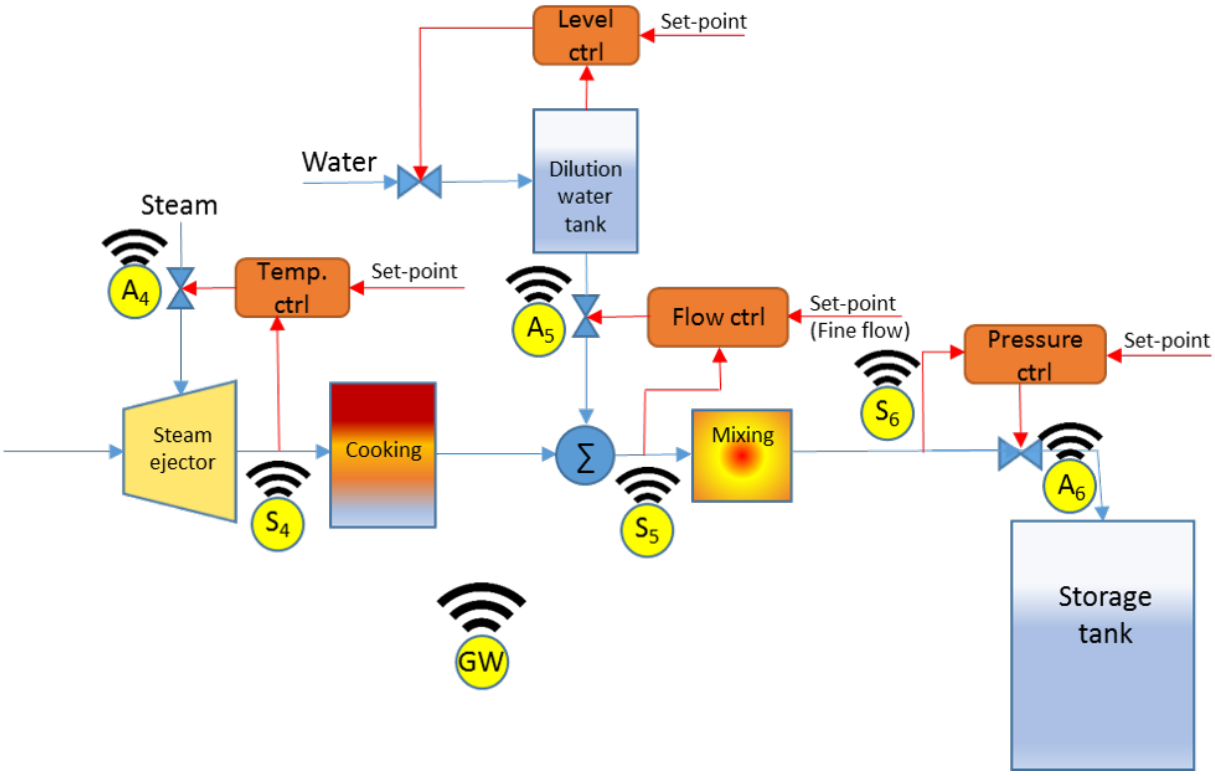

Figure 16. Block diagram of a starch cooker. Three control loops are installed with wireless actuators and wireless sensors. The level controller is a PI controller, the temperature controller is also a PI controller, and the pressure controller is a PID controller.

Figure 17. The environment where the wireless devices where installed. The picture shows a mixing tank where the flow of the slurry into the cooking process is measured. The gateway and the field devices were realized by assembling two off-the-shelf evaluation boards in an IP67 enclosure. A CAN bus IO from ABB (CI581) with analogue inputs and outputs, as well as digital counterparts, was connected to the field devices.

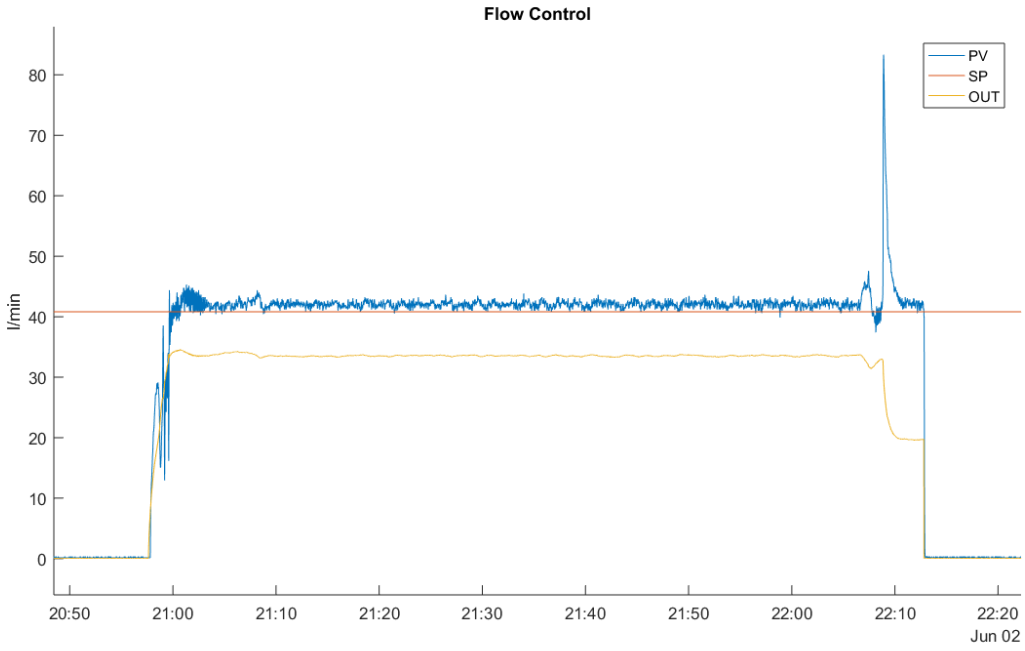

Figure 18. Performance of the flow controller during the starch cooking process. PV is the process value in l/min, SP is the set-point, and OUT is the output signal to the control valve in %. At the beginning of the batch sequence at 21:00, the flow controller aims to keep a water flow of 41 liters/minute. Shortly before 22:10, the level of the storage tank has reached the upper threshold such that the control valves to the storage tanks are closed and a cleaning process starts. The opening of the pressure valve (see also Figure 19) for cleaning acts as a flow disturbance. The cleaning process finished at 22:15 and the starch cooking system is ready for another batch as soon as the storage tank level reaches its lower threshold.

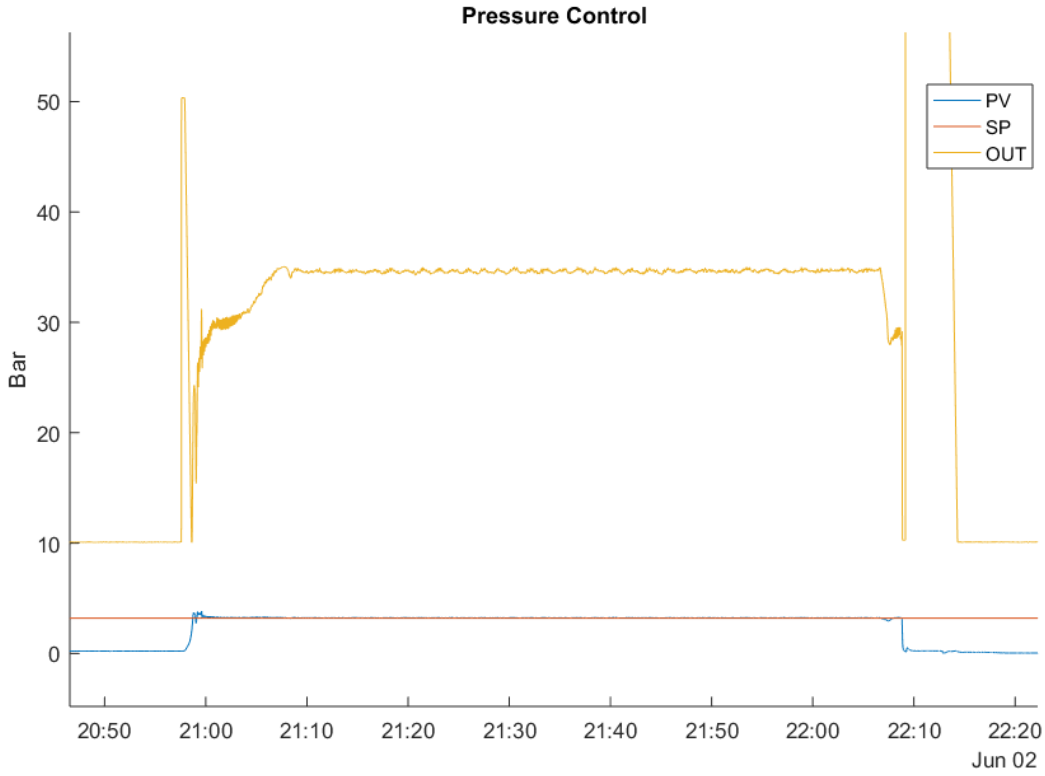

Figure 19. Performance of the pressure controller during the starch cooking process. PV is the process value in Bar, SP is the set-point, and OUT is the output signal to the control valve in %. At the beginning of the batch process at 21:00, the control valve of the pressure controller is opened to 50% to flush out remainders of starch from the previous batch. Then, the pressure controller aims to maintain a pressure of 3.3 Bar while heating the boiler (see Figure 20). Once the batch process is completed just before 22:10, the cleaning process starts by opening the pressure valve and finishes at 22:15.

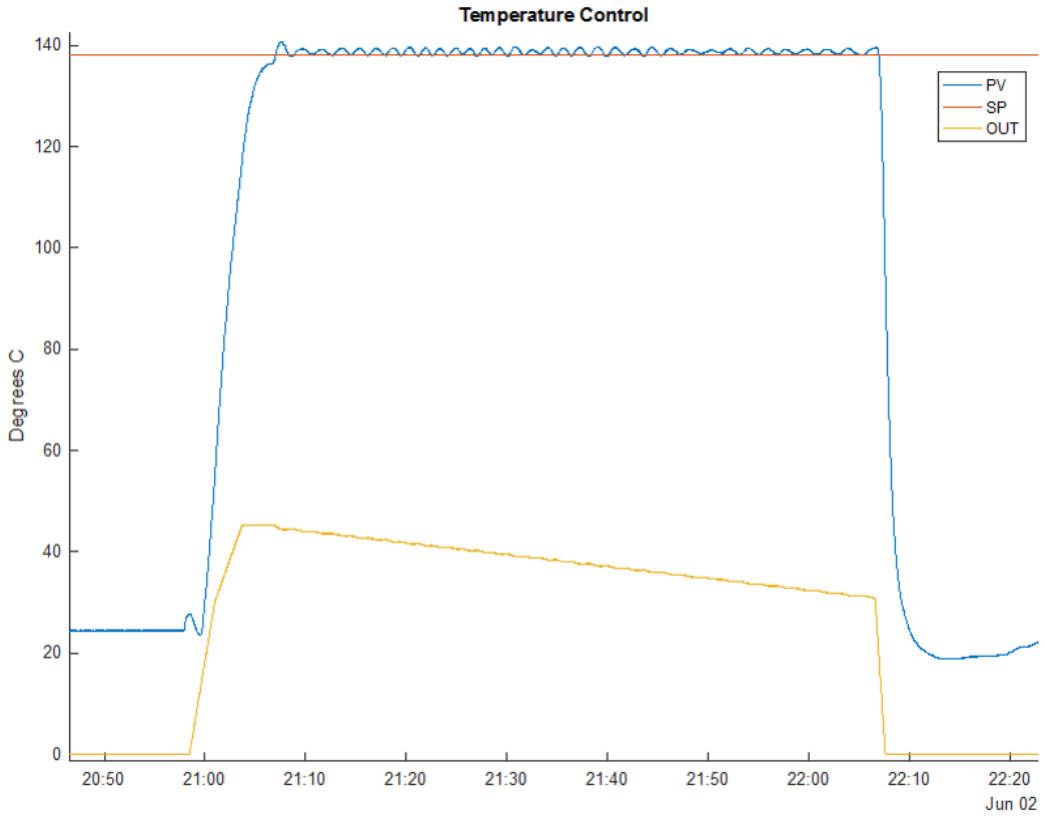

Figure 20. Performance of the temperature controller during the starch cooking process. PV is the process value in Celsius, SP is the set-point, and OUT is the output signal to the control valve in %. At the beginning of the batch process around 21:00, the boiler starts to heat with steam using a ramp in the output of the control valve. When reaching the desired temperature of 138 degrees Celsius shortly after 21:00, the temperature controller is enabled to maintain the temperature.

Sidebar: Summary

Wireless sensor networks are to a growing extent being deployed in process industry, but there are still several issues that need to be addressed for this technology to reach its full potential. This paper describes some of the main challenges in next generation process control, with an architecture based on distributed control nodes connected to a real-time data bus over wireless and wired networks. A case study focused on one of the starch cooker processes of the Iggesund pulp and paperboard mill in Sweden is used to illustrate various challenges and solutions to sensing, communication, and control for emerging wireless process automation. Radio environment modeling, network protocol design, energy harvesting, and event-based control are discussed in some detail. Experimental tests on the starch cooker during normal production over five consecutive days indicates that it is sometimes possible to replace wired control systems with wireless in complex industrial environments.

Sidebar: Iggesund Mill History

Iggesund Mill's origin is found in the forests outside Hudiksvall in Sweden, more specifically in the small town of Iggesund. The society has a long history, already in the middle of the 16th century there were small industries in and around the town. In 1685 the trader and chief commissioner, Isak Breant, received a license to construct an ironworks in the lower part of Iggesundsån (Iggesund River). Soon thereafter the production was started at the plant.

However, in the upper part of Iggesundsån there was already a paper mill, Östanå paper mill. Iggesund Mill bought this paper mill in 1771. The Östanå paper mill was the first in the world to try to produce paper from sawdust and wood, but the experiments never reached beyond the experimental stage and in 1842 the paper mill burnt down.

In 1869, Baron Gustav Tamm took over as owner of Iggesund Mill and he was able to construct a large sawmill which he started to build in 1870. In addition to the purchase of Östanå paper mill, this marks the first transition from a refined iron industry to a wood industry. Between the years 1915-1917, a cellulose factory was built on a new site further away from Iggesundsån. For a photo from 1916, see Figure S1. In 2017, the company celebrated that the factory had been 100 years in the same location as today.

Today, Iggesund Mill is best known for its white premium cardboard, but it was not until the beginning of the 1960s that they started making cardboard at the mill. Iggesund Mill was only the third manufacturer in the world which installed a carton machine with the new modern technology; the other two were previously in Australia and England. In 1963 the first cardboard machine at the Iggesund Mill was started. The second cardboard machine was started in 1971.

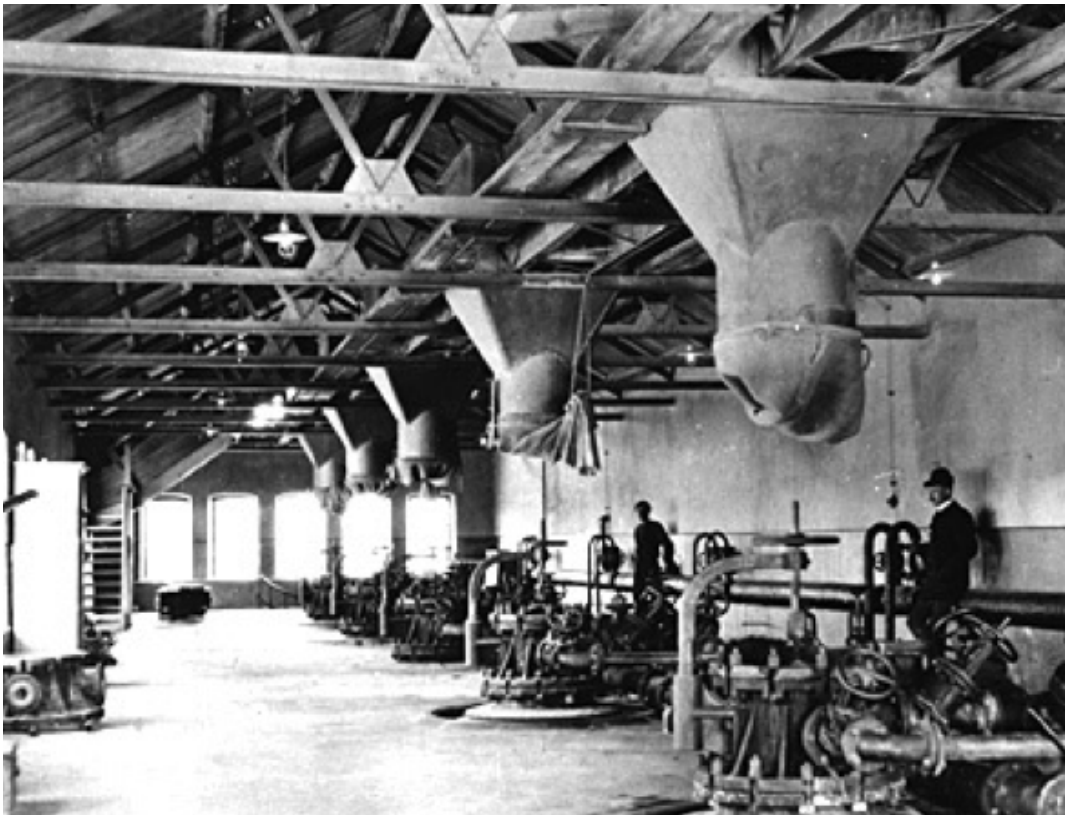

Figure S1. The photo is taken in the production room of the old sulphite digester. The house has long been demolished and today there are no traces left of it. At that time when the photo was taken 1916, the sulphite process was used to produce pulp. Today, the process has changed and instead it uses the sulphate process to achieve a better quality and whiteness of the pulp.

Figure S2. Aerial view of Iggesunds Bruk from 1940. At that time, Iggesunds Bruk was only a pulp mill. The first cardboard machine was started in 1963 and with this Iggesunds Bruk became both a producer of pulp and cardboard. The factory area is still in the same location as when the first pulp mill started in 1916.

Figure S3. Iggesund Paperboard's first cardboard machine called KM1 and is still in use, but since the photo was taken in 1968, it has been rebuilt several times. The photo is taken so that you see the reeling of the cardboard and in the middle of the picture you see the coating stations. At the far left of the picture, the drying unit of the cardboard machine is visible.

Sidebar: Radio Model Selection

Radio links of the kind depicted in Figure 6 can be modeled as a mixture probability density function (pdf) with M components,

$$p(y|\varphi) = \sum_{i=1}^{M} P_i p(y|\theta_i), \tag{S1}$$

where y is the underlying continuous variable representing power, $P_1, ..., P_M$ are mixture probabilities satisfying $\sum_i P_i = 1$, and $p(y|\theta_i)$ is the pdf of the i:th mixture component that is described by the parameter vector θ_i, and $\varphi = \{\theta_1, ..., \theta_M, P_1, ..., P_M\}$.

The corresponding discrete distribution for quantized data is obtained by integration over the user selected bin intervals, say I_k, $\forall k$, that is,

$$P(k|\varphi) \triangleq Pr(y \in I_k|\varphi) = \int_{y \in I_k} p(y|\varphi)dy \quad ; \quad \forall k \ . \tag{S2}$$

As will be explained below, see also Figure 8, an individual mixture component, $p(y|\theta_i)$, is preferably modeled as either purely Gamma (G), log-Normal (LN), or Gamma log-Normal (GLN) distributed. The G distribution in the power domain is given by

$$p_G(y) = \frac{m^m \exp\left(m\frac{y-\bar{y}}{\mu}\right) \exp\left(-m \exp\left(\frac{y-\bar{y}}{\mu}\right)\right)}{\mu\Gamma(m)}, \tag{S3}$$

where $\bar{y}$ is the mean, μ is a constant, and m is the Nakagami-m parameter. Hence, the pure G component can be parameterized by $\theta_i = (\bar{y}_i, m_i)$.

The compound GLN fading model arises for a power gain that is the product of two independent factors where one is G distributed and one is LN distributed. Expressed in dB, the LN distribution is

$$p_{LN}(y) = \frac{1}{(2\pi)^{1/2}\sigma} \exp\left(-\frac{y^2}{2\sigma^2}\right) \tag{S4}$$

where σ is the standard deviation and where we, without loss of generality, have set the mean to zero. Expressed in y, the above mentioned product becomes a sum of independent variables and the resulting pdf for this sum, $p_{GLN}(y)$, is given by the convolution $p_{GLN}(y) = p_G(y) * p_{LN}(y)$. The GLN component is thus parameterized by the tuple $\theta_i = (\bar{y}_i, m_i, \sigma_i)$.

Sidebar: Data Generation Model

Let $\mathbf{x}_l = [x_{l,1}, ..., x_{l,T}]$ denote T scalar Received Signal Strength (RSS) measurements from the lth link. The observations in $\mathbf{x}_l$ are assumed to be generated by a two state Hidden Markov Model (HMM), where $z_{l,t} \in [0,\ 1]$ denote the state of the model that is associated with the lth time series at time t. As described in more detail below, $z_{l,t}$ parameterizes the generative distribution of $x_{l,t}$. The state sequence $\mathbf{z}_l = [z_{l,1}, ..., z_{l,T}]$ is generated by a Markov model with transition probabilities, $Q_l = \{q_{l,i,j} : i, j \in [1, 2]\}$, where $q_{l,i,j}$ denotes the probability,

$$q_{l,i,j} = P(z_{l,t+1} = j | z_{l,t} = i). \tag{S5}$$

The initial state distribution is denoted $\boldsymbol{\pi}_l = \{\pi_{l,i} : i \in [1, 2]\}$ where,

$$\pi_{l,i} = P(z_{l,1} = i). \tag{S6}$$

Each state generates observations from an AR process, such that

$$x_{l,t} = \mathbf{x}_{l,t-1:t-v}\mathbf{a}'_{l,z_{l,t}} + e_{l,t}, \tag{S7}$$

where $\mathbf{a}_{l,z} = [a_{l,z,1}, ..., a_{l,z,v}]$ are the AR-coefficients for state z, v is the order of the process, and $e_{l,t}$ is independent, zero-mean, Gaussian noise with variance σ^2_{l,z_t}.

We choose to label the states so that state $z_{l,t} = 1$ corresponds to the more volatile fading state, for example, $\sigma^2_{l,1} > \sigma^2_{l,0}$. Also, we fix $v = 2$ which results in a satisfactory segmentation performance for all time series. Let $\Lambda_l = \{Q_l, \boldsymbol{\pi}_l, \mathbf{a}_l, \boldsymbol{\sigma}_l\}$ denote the collection of model parameters where $\mathbf{a}_l = \{\mathbf{a}_{l,z} : z \in [1, 2]\}$ and $\boldsymbol{\sigma}_l = \{\sigma^2_{l,z} : z \in [1, 2]\}$.

Estimation of model parameters

In [18], Rabiner outlined an iterative algorithm for computing the maximum likelihood estimate, $\hat{\Lambda}_l$, of the model parameters,

$$\hat{\Lambda}_l = \arg\max_{\Lambda_l} P(\mathbf{x}_l | \Lambda_l), \tag{S8}$$

and we refer the interested reader to the original work for details on the algorithm.

Since the inference objective is to use the HMM to detect changes in volatility, the RSS measurements were preprocessed with a bandpass filter with cutoff frequencies at $[\frac{1}{2},\ 2]$ Hz. This eliminated slow varying trends and measurement noise from $\mathbf{x}_l$ prior to estimation of $\hat{\Lambda}_l$.

Inference of the state sequence

Conditioned on $\hat{\Lambda}_l$, the most likely state sequence, $\hat{\mathbf{z}}_l = [\hat{z}_{l,1}, ..., \hat{z}_{l,T}]$, is obtained by maximizing,

$$\hat{\mathbf{z}}_l = \arg\max_{\mathbf{z}_l} P(\mathbf{x}_l, \mathbf{z}_l | \hat{\Lambda}_l), \tag{S9}$$

and the solution can be computed using the Viterbi algorithm in [18].

Sidebar: Advances in Wireless Control

Along the development of wireless technology, industrial control by means of wireless communications has received much attention in both academia and industry. Recent research issues on control over wireless communications, especially in industrial automation systems, are summarized in [2], [5], [9], [S1]–[S4]. In [5], [S1], [S2], some communication protocols developed for industrial wireless communications such as WirelessHART [S5] and ISA-100 [S6] are discussed. In both WirelessHART and ISA-100, their hardware and protocols are specified by the standard of the low rate wireless personal area network, IEEE 802.15.4 [S7]. Some research focus on the implementation and design of control systems operating over the WirelessHART and ISA-100 communication protocols. In [S8], aperiodic control algorithms implemented over the IEEE 802.15.4 standard are proposed and evaluated on a double-tank laboratory experimental set-up. A network model which captures some important key aspects of the WirelessHART protocol – a multi-hop structure and TDMA communications with some different frequencies – is developed in [S9], [S10]. Emulation-based stability conditions are derived in [S9] and observer design under the impact of stochastic noise is discussed in [S10]. A model of control systems over a multi-hop network is proposed in [S11]. Based on this model, a co-design framework comprising both controller and network scheduling and routing is investigated in [S12]. In [S13], a co-design of LQG control and multi-hop network scheduling and routing and its reconfiguration is discussed. In [S14], a co-design of controller and network scheduling and routing is proposed for the WirelessHART standard, which is assumed to have network reconfiguration after a given period.

Wireless control is also studied in the context of networked control theory, which in general focuses on control problems under network-induced constraints such as delay, packet dropout, and channel capacity limitation [4], [S15]–[S17]. In [S18], LQG control with packet dropouts is considered. In [S19], a network with multiple sensors is considered while communication through intermediate nodes is studied in [S20]. LQG control with network induced delays and access constraints is investigated in [S21], [S22] where only a subset of sensors can access the controller. Network capacity is explicitly considered as a control theory- and information theory problem in [S23]–[S25].

Scheduling of data transmission of networked control systems has attracted attention to reduce the amount of communication. In [S26], [S27], a joint optimization problem is presented where the problem can be separated into an optimal estimation, an optimal control, and an optimal scheduling problem. Scheduling among multiple control loops with a shared communication network is proposed in [S28], [S29]. A prioritizing framework under limited channel slots is proposed in [S28], and a scheduling framework under a Media Access Control (MAC)-like

protocol is developed in [S29]. There is a lot of research considering sensor scheduling for state estimation. In [S30], a communication control scheme for Kalman filters is developed to improve the trade-off between estimation performance and communication cost. Optimal estimation with a multiple time-step cost is introduced in [S31]. The minimum mean square error (MMSE) estimation schedule can be obtained in some special cases. In [S32], the MMSE schedule between two sensors is obtained, which is extended to more sensors in [S33], [S34]. These works deal with a single-hop network, that is, every sensor can directly communicate with the remote estimator. A multi-hop network structure is considered in [S35]–[S37]. In [S36], [S37], the authors consider how to manage the control systems when the network environment is changed. In [S36], they propose a way to reconfigure the network under time-varying channel states.

Energy-aware control strategies over wireless communication is investigated in some previous work. Optimal sensor energy allocation is studied in [S38]–[S40]. Therein, the energy consumption is dealt with as a control variable, which determines the probability of packet loss. Energy allocation for state estimation is discussed in [S38], [S40]–[S42] and for optimal control in [S39]. Network control systems with energy harvesting sensors are considered in [S43]–[S45].

References

[S1] J. R. Moyne and D. M. Tilbury, "The emergence of industrial control networks for manufacturing control, diagnostics, and safety data," *Proc. IEEE*, vol. 95, no. 1, pp. 29–47, 2007.

[S2] C. Lu, A. Saifullah, B. Li, M. Sha, H. Gonzalez, D. Gunatilaka, C. Wu, L. Nie, and Y. Chen, "Real-time wireless sensor-actuator networks for industrial cyber-physical systems," *Proc. IEEE*, vol. 104, no. 5, pp. 1013–1024, 2016.

[S3] A. Willig, K. Matheus, and A. Wolisz, "Wireless technology in industrial networks," *Proc. IEEE*, vol. 93, no. 6, pp. 1130–1151, 2005.

[S4] A. A. Kumar S, K. Øvsthus, and L. M. Kristensen, "An industrial perspective on wireless sensor networks—a survey of requirements, protocols, and challenges," *IEEE Commun. Surv. Tutor.*, vol. 16, no. 3, pp. 1391–1412, 2014.

[S5] D. Chen, M. Nixon, and A. Mok, *WirelessHART: Real-Time Mesh Network for Industrial Automation*. Springer, 2010.

[S6] International Society of Automation, "Wireless systems for industrial automation: Process control and related applications, ISA-100.11a-2009," 2009.

[S7] IEEE 802.15.4 Standard: Wireless Medium Access Control (MAC) and Pysical Layer (PHY) Specification for Low-Rate Wireless Personal Area Networks (WPANs). [Online]. Available: http://www.ieee802.org/15/pub/TG4.html

[S8] J. Araújo, M. Mazo, A. Anta, P. Tabuada, and K. H. Johansson, "System architectures, protocols and algorithms for aperiodic wireless control systems," *IEEE Trans. Ind. Informat.*, vol. 10, no. 1, pp. 175–184, 2014.

[S9] A. I. Maass, D. Nešić, R. Postoyan, P. M. Dower, and V. S. Varma, "Emulation-based stabilisation of networked control systems over wirelesshart," in *Proc. IEEE Conf. Decision and Control*, 2017, pp. 6628–6633.

[S10] A. I. Maass, D. Nešic, R. Postoyan, and P. M. Dower, "Observer design for networked control systems implemented over WirelessHART," in *Proc. IEEE Conf. Decision and Control*, 2018, pp. 2836–2841.

[S11] R. Alur, A. d'Innocenzo, K. H. Johansson, G. J. Pappas, and G. Weiss, "Compositional modeling and analysis of multi-hop control networks," *IEEE Trans. Autom. Control*, vol. 56, no. 10, pp. 2345–2357, 2011.

[S12] F. Smarra, A. D'Innocenzo, and M. D. Di Benedetto, "Optimal co-design of control, scheduling and routing in multi-hop control networks," in *Proc. IEEE Conf. Decision and Control*, 2012, pp. 1960–1965.

[S13] T. Iwaki and K. H. Johansson, "LQG control and scheduling co-design for wireless sensor and actuator networks," in *Proc. IEEE Workshop Signal Processing Advances in Wireless Communications*, 2018.

[S14] G. D. Di Girolamo and A. D'Innocenzo, "Codesign of controller, routing and scheduling in wirelesshart networked control systems," *Int. J. Robust Nonlin.*, 2019.

[S15] W. Zhang, M. S. Branicky, and S. M. Phillips, "Stability of networked control systems," *IEEE Control Syst. Mag.*, vol. 21, no. 1, pp. 84–99, 2001.

[S16] L. Schenato, B. Sinopoli, M. Franceschetti, K. Poolla, and S. S. Sastry, "Foundations of control and estimation over lossy networks," *Proc. IEEE*, vol. 95, no. 1, pp. 163–187, 2007.

[S17] W. M. H. Heemels, A. R. Teel, N. Van de Wouw, and D. Nesic, "Networked control systems with communication constraints: Tradeoffs between transmission intervals, delays and performance," *IEEE Trans. Autom. Control*, vol. 55, no. 8, pp. 1781–1796, 2010.

[S18] V. Gupta, B. Hassibi, and R. M. Murray, "Optimal LQG control across packet-dropping links," *Syst. Control Lett.*, vol. 56, no. 6, pp. 439–446, 2007.

[S19] V. Gupta, N. C. Martins, and J. S. Baras, "Optimal output feedback control using two remote sensors over erasure channels," *IEEE Trans. Autom. Control*, vol. 54, no. 7, pp. 1463–1476, 2009.

[S20] V. Gupta, A. F. Dana, J. P. Hespanha, R. M. Murray, and B. Hassibi, "Data transmission over networks for estimation and control," *IEEE Trans. Autom. Control*, vol. 54, no. 8, pp. 1807–1819, 2009.

[S21] D. Hristu-Varsakelis and L. Zhang, "LQG control of networked control systems with access constraints and delays," *Int. J. Control*, vol. 81, no. 8, pp. 1266–1280, 2008.

[S22] D. Maity, M. H. Mamduhi, S. Hirche, K. H. Johansson, and J. S. Baras, "Optimal LQG control under delay-dependent costly information," *IEEE Contr. Syst. Lett.*, vol. 3, no. 1, pp. 102–107, 2019.

[S23] S. Tatikonda and S. Mitter, "Control under communication constraints," *IEEE Trans. Autom. Control*, vol. 49, no. 7, pp. 1056–1068, 2004.

[S24] G. N. Nair, F. Fagnani, S. Zampieri, and R. J. Evans, "Feedback control under data rate constraints: An overview," *Proc. IEEE*, vol. 95, no. 1, pp. 108–137, 2007.

[S25] T. Tanaka, P. M. Esfahani, and S. K. Mitter, "LQG control with minimum directed information: Semidefinite programming approach," *IEEE Trans. Autom. Control*, vol. 63, no. 1, pp. 37–52, 2018.

[S26] A. Molin and S. Hirche, "On LQG joint optimal scheduling and control under communication constraints," in *Proc. IEEE Conf. Decision and Control*, 2009, pp. 5832–5838.

[S27] ——, "On the optimality of certainty equivalence for event-triggered control systems," *IEEE Trans. Autom. Control*, vol. 58, no. 2, pp. 470–474, 2013.

[S28] ——, "Price-based adaptive scheduling in multi-loop control systems with resource constraints," *IEEE Trans. Autom. Control*, vol. 59, no. 12, pp. 3282–3295, 2014.

[S29] C. Ramesh, H. Sandberg, and K. H. Johansson, "Design of state-based schedulers for a network of control loops," *IEEE Trans. Autom. Control*, vol. 58, no. 8, pp. 1962–1975, 2013.

[S30] Y. Xu and J. P. Hespanha, "Estimation under uncontrolled and controlled communications in networked control systems," in *Proc. IEEE Conf. Decision and Control and European Control Conf.*, 2005, pp. 842–847.

[S31] Y. Mo, R. Ambrosino, and B. Sinopoli, "Sensor selection strategies for state estimation in energy constrained wireless sensor networks," *Automatica*, vol. 47, no. 7, pp. 1330–1338, 2011.

[S32] L. Shi and H. Zhang, "Scheduling two Gauss–Markov systems: An optimal solution for remote state estimation under bandwidth constraint," *IEEE Trans. Signal Process.*, vol. 60, no. 4, pp. 2038–2042, 2012.

[S33] D. Han, J. Wu, H. Zhang, and L. Shi, "Optimal sensor scheduling for multiple linear dynamical systems," *Automatica*, vol. 75, pp. 260–270, 2017.

[S34] S. Wu, X. Ren, S. Dey, and L. Shi, "Optimal scheduling of multiple sensors with packet length constraint," in *Proc. IFAC World Congress*, 2017, pp. 14 430–14 435.

[S35] D. E. Quevedo, A. Ahlén, and K. H. Johansson, "State estimation over sensor networks with correlated wireless fading channels," *IEEE Trans. Autom. Control*, vol. 58, no. 3, pp. 581–593, 2013.

[S36] A. S. Leong, D. E. Quevedo, A. Ahlén, and K. H. Johansson, "On network topology

reconfiguration for remote state estimation." *IEEE Trans. Autom. Control*, vol. 61, no. 12, pp. 3842–3856, 2016.

[S37] T. Iwaki, Y. Wu, J. Wu, H. Sansberg, and K. H. Johansson, "Wireless sensor network scheduling for remote estimation under energy constraints," in *Proc. IEEE Conf. Decision and Control*, 2017, pp. 3362–3367.

[S38] A. S. Leong, S. Dey, G. N. Nair, and P. Sharma, "Power allocation for outage minimization in state estimation over fading channels," *IEEE Trans. Signal Process.*, vol. 59, no. 7, pp. 3382–3397, 2011.

[S39] K. Gatsis, A. Ribeiro, and G. J. Pappas, "Optimal power management in wireless control systems," *IEEE Trans. Autom. Control*, vol. 59, no. 6, pp. 1495–1510, 2014.

[S40] X. Ren, J. Wu, K. H. Johansson, G. Shi, and L. Shi, "Infinite horizon optimal transmission power control for remote state estimation over fading channels," *IEEE Trans. Autom. Control*, vol. 63, no. 1, pp. 85–100, 2018.

[S41] A. S. Leong and S. Dey, "Power allocation for error covariance minimization in kalman filtering over packet dropping links," in *Proc. IEEE Conf. Decision and Control*, 2012, pp. 3335–3340.

[S42] D. E. Quevedo, A. Ahlén, A. S. Leong, and S. Dey, "On kalman filtering over fading wireless channels with controlled transmission powers," *Automatica*, vol. 48, no. 7, pp. 1306–1316, 2012.

[S43] A. Nayyar, T. Başar, D. Teneketzis, and V. V. Veeravalli, "Optimal strategies for communication and remote estimation with an energy harvesting sensor," *IEEE Trans. Autom. Control*, vol. 58, no. 9, pp. 2246–2260, 2013.

[S44] M. Nourian, A. S. Leong, and S. Dey, "Optimal energy allocation for kalman filtering over packet dropping links with imperfect acknowledgments and energy harvesting constraints," *IEEE Trans. Autom. Control*, vol. 59, no. 8, pp. 2128–2143, 2014.

[S45] S. Knorn, S. Dey, A. Ahlén, and D. E. Quevedo, "Optimal energy allocation in multi sensor estimation over wireless channels using energy harvesting and sharing," *IEEE Trans. Autom. Control*, 2019.

Sidebar: Advances in Event-based Control

Event-based sampling for the classical feedback control loop has been studied, often as a means to reduce communications among the system components without sacrificing performance, see, for example, [S46]–[S48], and the references therein.

Optimal estimation and LQG control with event-based sampling strategies are discussed by many researchers. The authors of [S49] offer a deterministic event-based scheduler by using feedback from the estimator. A stochastic schedule is proposed in [S50]. With a similar setup, a scheduling framework where the transmissions are invoked by the estimation error covariance is proposed in [S51]. In [S52], packet dropouts are considered for covariance-based state estimation. These works are then extended to LQG control problems in [S53]. In [S54], a TDMA-like time-triggered schedule as well as a CSMA-like event-triggered schedule with random or dynamic scheduler are analyzed. Multi-hop networks are explicitly considered in some studies. LQG control with event-based sampling is investigated in [S27], where an optimal design of the controller and the event-triggering law is obtained. The trade-off between LQG control performance and communication load for stochastic event-based control is discussed in [S55]. LQG control where the event-based communication is performed over WiFi is considered in [S56].

To implement event-based control strategies into industrial control loops, event-based PID control has been considered, for example, in [21], [22], [27], [S57]–[S60]. The works include both academic and industrial perspectives. As presented in [21], event-based PID control can significantly reduce the communication effort with only a slight or no degradation in control performance, which has motivated the process industry to use event-based PID control [28]. In [24], [25], event-based PID control is evaluated at an industrial paper mill plant in Iggesund. Some practical problems when introducing event-based PI control are discussed in [26], [27], [S59]. In [27], it is shown that event-based sampling may result in a sticking effect or stationary large oscillations. To overcome these problems, [27] proposes PIDPLUS [S61]–[S63]. The asymptotic stability conditions are derived with a relative threshold policy in [S59]. Furthermore, [26], [S60], [S64], [S65] focus on actuator saturation for event-based control. In fact, the stability region is influenced by the use of event-based control. In [26], it is shown that an anti-windup technique can significantly improve the performance for event-based control systems saturation. The authors of [S65] introduce an event-based anti-windup scheme. In [S60], the authors consider a zero-order hold between the controller and the actuator and they derive asymptotic stability conditions subject to actuator saturation. Other PID controller design problems are considered in [S58], [S59]. In [S58], the authors introduce an LQ control design problem with event-based sampling. PI control synthesis with a relative threshold strategy is

proposed in [S59].

References

[S46] W. M. H. Heemels, J. Sandee, and P. van den Bosch, "Analysis of event-driven controllers for linear systems," *Int. J. Control*, vol. 81, no. 4, pp. 571–590, 2008.

[S47] J. Lunze and D. Lehmann, "A state-feedback approach to event-based control," *Automatica*, vol. 46, no. 1, pp. 211–215, 2010.

[S48] W. M. H. Heemels, K. H. Johansson, and P. Tabuada, "An introduction to event-triggered and self-triggered control," in *Proc. IEEE Conf. Decision and Control*, 2012, pp. 3270–3285.

[S49] J. Wu, Q.-S. Jia, K. H. Johansson, and L. Shi, "Event-based sensor data scheduling: Trade-off between communication rate and estimation quality," *IEEE Trans. Autom. Control*, vol. 58, no. 4, pp. 1041–1046, 2013.

[S50] D. Han, Y. Mo, J. Wu, S. Weerakkody, B. Sinopoli, and L. Shi, "Stochastic event-triggered sensor schedule for remote state estimation," *IEEE Trans. Autom. Control*, vol. 60, no. 10, pp. 2661–2675, 2015.

[S51] S. Trimpe and R. D'Andrea, "Event-based state estimation with variance-based triggering," *IEEE Trans. Autom. Control*, vol. 59, no. 12, pp. 3266–3281, 2014.

[S52] A. S. Leong, S. Dey, and D. E. Quevedo, "Sensor scheduling in variance based event triggered estimation with packet drops," *IEEE Trans. Autom. Control*, vol. 62, no. 4, pp. 1880–1895, 2017.

[S53] A. S. Leong, D. E. Quevedo, T. Tanaka, S. Dey, and A. Ahlén, "Event-based transmission scheduling and LQG control over a packet dropping link," in *Proc. IFAC World Congress*, 2017, pp. 8945–8950.

[S54] M. Xia, V. Gupta, and P. J. Antsaklis, "Networked state estimation over a shared communication medium," *IEEE Trans. Autom. Control*, vol. 62, no. 4, pp. 1729–1741, 2017.

[S55] B. Demirel, A. S. Leong, V. Gupta, and D. E. Quevedo, "Trade-offs in stochastic event-triggered control," *IEEE Trans. Autom. Control*, vol. 62, no. 6, pp. 2973–2980, 2018.

[S56] M. Pezzutto, F. Tramarin, S. Dey, and L. Schenato, "Snr-triggered communication rate for lqg control over wi-fi," in *IEEE Conf. Decision and Control*, 2018, pp. 1725–1730.

[S57] S. Reimann, W. Wu, and S. Liu, "PI control and scheduling design for embedded control systems," in *Proc. IFAC World Congress*, 2014, pp. 11 111–11 116.

[S58] J. G. Silva Jr., W. F. Lages da, and D. Sbarbaro, "Event-triggered PI control design." in *Proc. IFAC World Congress*, 2014, pp. 6947–6952.

[S59] S. Reimann, D. H. Van, S. Al-Areqi, and S. Liu, "Stability analysis and PI control synthesis

under event-triggered communication," in *Proc. European Control Conf.*, 2015, pp. 2174–2179.

[S60] L. Moreira, L. Groff, J. G. da Silva, and S. Tarbouriech, "Event-triggered PI control for continuous plants with input saturation," in *Proc. American Control Conf.*, 2016, pp. 4251–4256.

[S61] J. Song, A. K. Mok, D. Chen, M. Nixon, T. Blevins, and W. Wojsznis, "Improving PID control with unreliable communications," in *Proc. ISA EXPO Technical Conf.*, 2006, pp. 17–19.

[S62] O. Kaltiokallio, L. M. Eriksson, and M. Bocca, "On the performance of the PIDPLUS controller in wireless control systems," in *Proc. Mediterranean Conf. Control and Automation*, 2010, pp. 707–714.

[S63] T. Blevins, M. Nixon, and W. Wojsznis, "PID control using wireless measurements," in *Proc. American Control Conf.*, 2014, pp. 790–795.

[S64] D. Lehmann, G. A. Kiener, and K. H. Johansson, "Event-triggered PI control: Saturating actuators and anti-windup compensation," in *Proc. IEEE Conf. Decision and Control*, 2012, pp. 6566–6571.

[S65] D. Lehmann and K. H. Johansson, "Event-triggered PI control subject to actuator saturation," in *Proc. IFAC Conf. Advances in PID Control*, 2012, pp. 430–435.

Biography

Anders Ahlén is full professor and holds the chair in Signal Processing at Uppsala University where he is the head of the Signals and Systems Division of The Department of Engineering Sciences. He received the PhD degree in Automatic Control from Uppsala University. He was with the Systems and Control Group, Uppsala University from 1984-1992 as an Assistant and Associate Professor in Automatic Control. During 1991 he was a visiting researcher at the Department of Electrical and Computer Engineering, The University of Newcastle, Australia. He has been a visiting professor at the same university several times since 2008. During 2001-2004 he was the CEO of Dirac Research AB, a company offering state-of-the-art audio signal processing solutions. Since 2005 he has been the chairman of the Board of Directors of the same company. His research interest includes Signal Processing, Communications and Control, and is currently focused on Signal Processing for Wireless Communications, Wireless Sensor Networks, Wireless Control, and Audio Signal Processing. From 1998 to 2004 he was the Editor of Signal and Modulation Design for the IEEE Transactions on Communications. He is a Senior Member of IEEE and a member of The Royal Society of Sciences at Uppsala.

Johan Åkerberg is a principal scientist at ABB Corporate Research in Sweden. He received the MSc and PhD degree in Computer Science and Engineering from Mälardalen University, Sweden. He has 25 years of experience within ABB in various positions such as global research area coordinator, R&D project manager, automation lead engineer, industrial communication specialist and product manager.

Markus Eriksson is currently working towards a Ph.D. degree in electrical engineering with specialization in signal processing at the Signals and Systems Division of the Department of Engineering Sciences, Uppsala University. He has a professional background as a software developer at Scania CV in Södertälje, Sweden. His research interests are in the fields of signal processing, in particular change point detection and embedded systems.

Alf Isaksson received the M.Sc. in Computer Engineering and Ph.D. in Automatic Control both from Linköping University in 1983 and 1988 respectively. After graduating he stayed at Linköping University until 1991 as an Assistant Professor. From 1991 to 1992 he spent one year as a Research Associate at The University of Newcastle, Australia. Returning to Sweden in 1992 he moved to the Royal Institute of Technology (KTH) in Stockholm,

where eventually in 1999 he was promoted to full Professor. In 2001 he made the shift from academic to industrial research and joined ABB Corporate Research in Västerås, Sweden. After a specialist career culminating in a promotion to Corporate Research Fellow in 2009, he was from 2014 until March this year Group Research Area Manager with the responsibility of internally funding all research in Control at all of ABB's 7 research centers world-wide. At the same time, he still kept a connection to the academic world as Adjunct Professor in Automatic Control at Linköping University 2006-2015, where he was leading a Process Industry Center from 2009 to 2012. He is currently involved in creating a new global entity called ABB Future Labs focusing on Artificial Intelligence and Autonomous Systems. He is a Senior Member of IEEE and a member of The Royal Swedish Academy of Engineering Sciences.

Takuya Iwaki received the B.E. and M.E. degrees from Tokyo Institute of Technology, Tokyo, Japan, in 2009 and 2012, respectively. He was with JGC Corporation, Yokohama, Japan, as a process control engineer from 2012 to 2016. He is currently a doctoral student at the School of Electrical Engineering and Computer Science, KTH Royal Institute of Technology, Stockholm, Sweden. His main research interests include control and estimation over wireless communication, and their application to industrial process control systems.

Karl Henrik Johansson is Professor at the School of Electrical Engineering and Computer Science, KTH Royal Institute of Technology. He received the MSc and PhD degrees from Lund University. He has held visiting positions at UC Berkeley, Caltech, NTU, HKUST Institute of Advanced Studies, and NTNU. His research interests are in networked control systems, cyber-physical systems, and applications in transportation, energy, and automation networks. He has served on the IEEE Control Systems Society Board of Governors, the IFAC Executive Board, and the European Control Association Council. He has received several best paper awards and other distinctions from IEEE and ACM. He has been awarded Distinguished Professor with the Swedish Research Council and Wallenberg Scholar with the Knut and Alice Wallenberg Foundation. He has received the Future Research Leader Award from the Swedish Foundation for Strategic Research and the triennial Young Author Prize from IFAC. He is Fellow of the IEEE and the Royal Swedish Academy of Engineering Sciences, and he is IEEE Distinguished Lecturer.

Steffi Knorn received the Dipl.Ing. in 2008 from the University of Magdeburg, Germany, and the Ph.D. from the Hamilton Institute at the National University of Ireland Maynooth, Ireland, in 2013. In 2013 she was a research academic at the Centre for Complex Dynamic

Systems and Control at the University of Newcastle, Australia. Since 2014 she is with the Signals and Systems Division at Uppsala University, Sweden. Dr. Knorn's research interests include stability analysis and controller design for marginally stable two-dimensional systems, port-Hamiltonian systems, string stability and scalability of vehicle platoons, distributed control, multi-sensor estimation, and energy harvesting and energy sharing in wireless networks.

Thomas Lindh works as an automation engineer at the Maintenance Technology Development, Iggesund Mill, Iggesund Paperboard. He has 20 years of experience in pulp and paper industry. The first 9 years as an instrument technician and the last 11 years as an automation engineer. He is the system administrator for the DCS system at the board machines.

Henrik Sandberg is Professor at the Division of Decision and Control Systems, KTH Royal Institute of Technology, Stockholm, Sweden. He received the M.Sc. degree in engineering physics and the Ph.D. degree in automatic control from Lund University, Lund, Sweden, in 1999 and 2004, respectively. From 2005 to 2007, he was a Post-Doctoral Scholar at the California Institute of Technology, Pasadena, USA. In 2013, he was a visiting scholar at the Laboratory for Information and Decision Systems (LIDS) at MIT, Cambridge, USA. He has also held visiting appointments at the Australian National University and the University of Melbourne, Australia. His current research interests include security of cyber-physical systems, power systems, model reduction, and fundamental limitations in control. Dr. Sandberg was a recipient of the Best Student Paper Award from the IEEE Conference on Decision and Control in 2004, the Ingvar Carlsson Award from the Swedish Foundation for Strategic Research in 2007, and a Consolidator Grant from the Swedish Research Council in 2016. He has served on the editorial board of IEEE Transactions on Automatic Control and is currently Associate Editor of the IFAC Journal Automatica.